JACS
JOURNAL OF THE AMERICAN CHEMICAL SOCIETY
Article
pubs.acs.org/JACS

Room Temperature Dehydrogenation of Ethane, Propane, Linear Alkanes C4−C8, and Some Cyclic Alkanes by Titanium−Carbon Multiple Bonds

Marco G. Crestani, Anne K. Hickey, Xinfeng Gao, Balazs Pinter, Vincent N. Cavaliere, Jun-Ichi Ito, Chun-Hsing Chen, and Daniel J. Mindiola*,†

Department of Chemistry, Indiana University, Bloomington, Indiana 47405, United States

Supporting Information

ABSTRACT: The transient titanium neopentylidyne, [(PNP)Ti≡C^{t}Bu] (**A**; PNP$^-$≡N[2-P^{i}Pr$_2$-4-methylphenyl]$_2^-$), dehydrogenates ethane to ethylene at room temperature over 24 h, by sequential 1,2-CH bond addition and β-hydrogen abstraction to afford [(PNP)Ti(η^2-H$_2$C=CH$_2$)(CH$_2$^{t}Bu)] (**1**). Intermediate **A** can also dehydrogenate propane to propene, albeit not cleanly, as well as linear and volatile alkanes C$_4$−C$_6$ to form isolable α-olefin complexes of the type, [(PNP)Ti(η^2-H$_2$C=CHR)(CH$_2$^{t}Bu)] (R = CH$_3$ (**2**), CH$_2$CH$_3$ (**3**), ^{n}Pr (**4**), and ^{n}Bu (**5**)). Complexes **1**−**5** can be independently prepared from [(PNP)Ti=CH^{t}Bu(OTf)] and the corresponding alkylating reagents, LiCH$_2$CHR (R = H, CH$_3$(unstable), CH$_2$CH$_3$, ^{n}Pr, and ^{n}Bu). Olefin complexes **1** and **3**−**5** have all been characterized by a diverse array of multinuclear NMR spectroscopic experiments including ^{1}H−^{31}P HOESY, and in the case of the α-olefin adducts **2**−**5**, formation of mixtures of two diastereomers (each with their corresponding pair of enantiomers) has been unequivocally established. The latter has been spectroscopically elucidated by NMR via C−H coupled and decoupled ^{1}H−^{13}C multiplicity edited gHSQC, ^{1}H−^{31}P HMBC, and dqfCOSY experiments. Heavier linear alkanes (C$_7$ and C$_8$) are also dehydrogenated by **A** to form [(PNP)Ti(η^2-H$_2$C=CH^{n}Pentyl)(CH$_2$^{t}Bu)] (**6**) and [(PNP)Ti(η^2-H$_2$C=CH^{n}Hexyl)(CH$_2$^{t}Bu)] (**7**), respectively, but these species are unstable but can exchange with ethylene (1 atm) to form **1** and the free α-olefin. Complex **1** exchanges with D$_2$C=CD$_2$ with concomitant release of H$_2$C=CH$_2$. In addition, deuterium incorporation is observed in the neopentyl ligand as a result of this process. Cyclohexane and methylcyclohexane can be also dehydrogenated by transient **A**, and in the case of cyclohexane, ethylene (1 atm) can trap the [(PNP)Ti(CH$_2$^{t}Bu)] fragment to form **1**. Dehydrogenation of the alkane is not rate-determining since pentane and pentane-d_{12} can be dehydrogenated to **4** and **4**-d_{12} with comparable rates (KIE = 1.1(0) at ∼29 °C). Computational studies have been applied to understand the formation and bonding pattern of the olefin complexes. Steric repulsion was shown to play an important role in determining the relative stability of several olefin adducts and their conformers. The olefin in **1** can be liberated by use of N$_2$O, organic azides (N$_3$R; R = 1-adamantyl or SiMe$_3$), ketones (O=CPh$_2$; 2 equiv) and the diazoalkane, N$_2$CHtolyl$_2$. For complexes **3**−**7**, oxidation with N$_2$O also liberates the α-olefin.

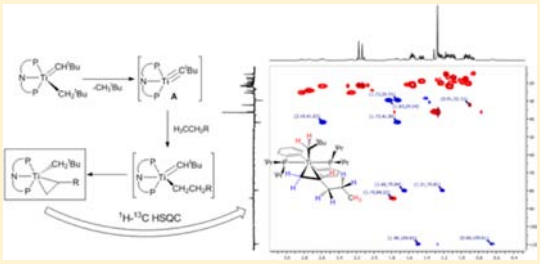

INTRODUCTION

In the face of a world energy crisis,[1] spurred by rising global temperatures and dwindling accessible petroleum reserves,[2] the quest for new methods to better convert vast resources such as natural gas into more useful commodity reagents is an attractive research endeavor.[2−4]The chemistry of alkanes has been one of the most intriguing challenges to chemists in the 20th century,[4,5] but despite research efforts few examples for selective conversions of the most volatile alkanes[6] (and hence the most abundant) are known.[7,8] Consequently, one of the most important challenges facing chemists, both fundamentally and practically speaking, is the efficient and mild activation and functionalization of the major components of natural gas: methane,[8t,9] ethane, and other alkanes; many of which constitute some of the most kinetically inert components, not ideal for use as liquid fuels.[10]

In this context, large-scale industrial processes, such as steam reforming,[11] steam cracking,[12] and Fischer−Tropsch,[3d,13] are vastly important given the ever growing world energy demand in order to convert volatile alkanes to more synthetically useful products such as liquid fuels or unsaturated compounds,[14] but in all cases these transformations are thoroughly energy and capital intensive.

Steam cracking is especially useful worldwide for these purposes, being a chief-industrial transformation that converts vast resources such as ethane to ethylene and other more reactive hydrocarbons.[15,16] In this process, a stream of light alkanes (ethane, propane, butane) are heated using high velocities and diluted with steam to elicit C−C bond homolysis. The resulting alkanes undergo a series of radical reactions that

Received: June 15, 2013
Published: August 26, 2013

dx.doi.org/10.1021/ja4060178 | J. Am. Chem. Soc. 2013, 135, 14754−14767

Scheme 1. Divergent Reactivity of *n*-Hexane with Pincer-Iridium Complexes: Dehydroaromatization (above) and Alkane Metathesis via Tandem Dehydrogenation/Olefin Metathesis (below)

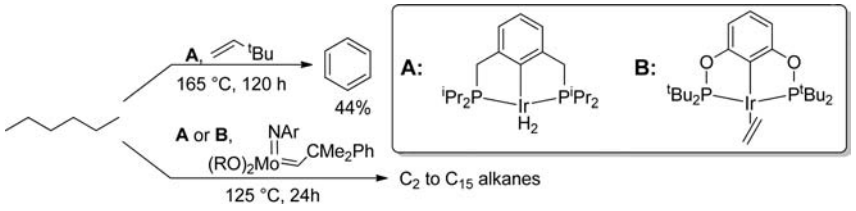

ultimately lead to the corresponding olefins (ethylene, propene, butenes, etc.) and a fraction of dienes (e.g., 1,3-butadiene). However, the process, which accounts for over 65% of ethylene production in the U.S. and over 90% of ethylene production in North America, requires temperatures in excess of 800 °C and current technology, on average, produces 1−3 tons of CO_2 per ton of ethylene formed.[15]

As a result, finding a method that would selectively convert alkanes to alkenes under mild conditions[10b,17] would be of significant practical utility, since an olefin such as ethylene is the second-most produced chemical in the world after sulfuric acid. Notably, ethylene is also the starting material for other industrially important raw materials such as 1,2-dichloroethane, ethylene oxide, and styrene among many other products. Terminal olefins such as propene, 1-butene, and 1-hexene are equally important, but their low-yield production in the steam cracking process, coupled with the energy needed to produce these monomers, has triggered the pursuit of alternative pathways as a result of the rising costs of crude oil.

One attractive transformation for mildly converting linear alkanes to olefins is the process denoted transfer dehydrogenation.[9] Crabtree originally showed that low-valent and electron-poor diphosphino-iridium complexes could dehydrogenate cyclooctane, proceeding via a series of oxidative addition and β-hydride elimination steps.[8a] Due to the inherent endothermicity of this reaction, high temperatures and a sacrificial olefin must be used to abstract the dihydrogen equivalents.[18] Indeed, tandem methods based on olefin metathesis and concurrent hydrogenation that eliminate the requirement of a sacrificial olefin have been developed recently.[19] Organometallic catalysts incorporating iridium,[9,20] rhenium,[20] rhodium,[21] and ruthenium[22] have been developed for such methods, being highly active toward alkane dehydrogenation, in some cases with excellent selectivity.

To date, the most efficient and versatile catalyst is the pincer-iridium complex developed by Kaska,[23] Jensen,[24] and Goldman.[19] This catalyst system, [(PCP)IrH_2] (PCP$^-$ = 2,6-$(R_2PCH_2)_2C_6H_3$, R = ^{i}Pr or ^{t}Bu) has been shown to dehydrogenate cyclooctane with unprecedented turnover frequency (TOF) and turnover numbers (TON).[9] A variation of this complex also selectively converts linear alkanes such as *n*-octane to 1-octene, but prolonged exposure to the catalysis conditions converts the terminal olefins to the thermodynamically favored internal olefins.[9a] Another variation of ancillary ligand gave rise to dehydroaromatization of *n*-hexane, *n*-heptane, and *n*-octane to give benzene, toluene, and a mixture of *o*-xylene and ethylbenzene, respectively (Scheme 1).[25] One notable accomplishment of this catalyst architecture has been tandem catalysis with a Schrock-type olefin metathesis catalyst, which accomplishes an overall alkane metathesis cycle, converting *n*-hexane to an array of alkanes, C_2−C_{20} (Scheme 1).[19] While the current series of dehydrogenation catalysts has proven to be versatile and efficient, reactions that could operate under even milder conditions (especially using cheaper metals) are desirable, since the least reactive alkanes could be converted to their respective terminal olefin. Likewise, converting alkanes to terminal olefins without the need of a β-hydride elimination step would be attractive since the microscopic reverse step, migratory insertion of an olefin, would be avoided. Under conditions where allylic C−H bond activation is unfavorable,[26] this feature would block detrimental isomerization pathways of the terminal olefin to the more thermodynamically favored (but less synthetically useful) internal olefin.

In recent years, our group reported that the complex [(PNP)Ti=CH^{t}Bu($CH_2{}^t$Bu)] decays in solution with $t_{1/2}$ = 3.1 h at room temperature ($k_{avg} = 5 \times 10^{-5}$ s^{-1}) to generate an unprecedented transient and terminal titanium alkylidyne [(PNP)Ti≡C^{t}Bu] (**A**).[27] This complex then activates the C−H bond of benzene by 1,2-addition across the alkylidyne moiety to generate [(PNP)Ti=CH^{t}Bu(Ph)].[27] Later it was found that this complex could activate multiple sp^3 C−H bonds in $SiMe_4$, $Me_3SiC{\equiv}CSiMe_3$, $Me_3CC{\equiv}CCMe_3$, 1,3,5-$Me_3C_6H_3$ and MeC_6F_5 by virtue of (1) 1,2-CH bond addition, (2) α-hydrogen abstraction, and (3) tautomerization steps to yield [(PNP)Ti=CHR(CH_2R)] (R = $SiMe_3$, $SiMe_2C{\equiv}CSiMe_3$, $CMe_2C{\equiv}CCMe_3$, $C_6H_3Me_2$, C_6F_5), in an overall dehydrogenation process also referred to as an alkylidene-alkyl metathesis reaction (Scheme 2).[27b] Species **A** also activates a C−H bond of methane to generate [(PNP)Ti=CH^{t}Bu(CH_3)],[10] a relatively stable methyl complex that can undergo slow exchange with the neopentylidene ligand via a possible titanium methylidene species (Scheme 2). More recently, we extended

Scheme 2. Dehydrogenation of $SiMe_4$, $Me_3SiC{\equiv}CSiMe_3$, $Me_3CC{\equiv}CCMe_3$, 1,3,5-$Me_3C_6H_3$, $CH_3C_6F_5$, CH_4, and CH_3CH_3 by Transient A

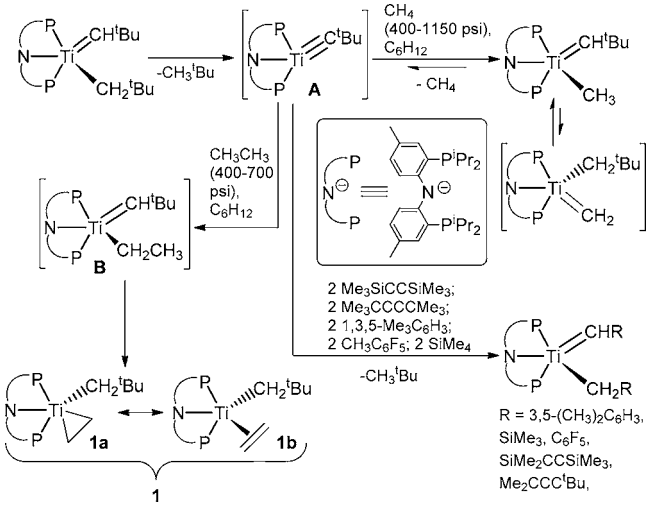

dx.doi.org/10.1021/ja4060178 | J. Am. Chem. Soc. 2013, 135, 14754−14767

the chemistry of **A** to the C−H activation of ethane which results in formation of an η^2-ethylene complex of the type, [(PNP)Ti(η^2−H_2C=CH_2)($CH_2{}^tBu$)] (**1**), by a stepwise double α,β C−H bond activation process.[28] Linear ethers can be also dehydrogenated by **A**, albeit in competition with a dehydroalkoxylation pathway.[29] In the current work we report the first complete and systematic study of the room temperature dehydrogenation of ethane, propane, and linear alkanes ranging from C_4−C_8 by **A**, to form terminal olefins exclusively. We combine a battery of NMR spectroscopic experiments and DFT to understand the structure of the olefin compounds formed in solution and showcase a new mechanism of alkane dehydrogenation that includes those of cyclohexane and methylcyclohexane; the first of which decays in solution via formation of an unstable titanium(II) species with concomitant release of cyclohexene. Reactivity studies involving the titanium olefin complexes are also presented.

RESULTS AND DISCUSSION

Synthesis of the Titanium-Olefin Complexes by Alkane Dehydrogenation. As shown in an earlier communication,[28] a cyclohexane (C_6H_{12}) solution of complex [(PNP)Ti=$CH^tBu(CH_2{}^tBu)$] under ethane pressure (400−700 psi), in a sealed, stainless steel reactor at room temperature for 24 h, gives rise to an η^2-ethylene complex, [(PNP)Ti(η^2-H_2C=CH_2)($CH_2{}^tBu$)] (**1**) (Scheme 2), on the basis of multinuclear and multidimensional NMR spectroscopy (vide infra). Complex **1** is formed in quantitative yield via a stepwise double α β C−H bond activation process through a titanium-neopentylidene-ethyl intermediate, [(PNP)Ti=CH^tBu-(C_2H_5)] (**B**) (Scheme 2). The structure of **1** can be described as a metallacyclopropane where significant backbonding with the olefin occurs (resonance **1a**), or by a canonical form having an ethylene-bound ligand that is purely a σ-donor (resonance **1b**) in accordance with the Dewar−Chatt−Duncanson model in metal-olefin bonding.[30] Complex **1** gradually decomposes above 65 °C releasing ethylene and forming a myriad of PNP-based products.

When [(PNP)Ti=$CH^tBu(CH_2{}^tBu)$] is treated with propane (120 psi) in cyclohexane, the propene complex [(PNP)Ti(η^2-H_2CCHCH_3)($CH_2{}^tBu$)] (**2**) is formed but not cleanly given the observation of other titanium products including free (PNP)H, when the mixture is gauged by $^{31}P\{^1H\}$ NMR spectroscopy (Scheme 3). Unlike **1**, complex **2** exists as a mixture of diastereomers in a 1:3 ratio due the asymmetry of the α-olefin, as well as the C_2 symmetric nature of the PNP ligand (the aryl moieties are not coplanar). Unfortunately complex **2** is unstable and undergoes decomposition over minutes, thus preventing us from fully characterizing this species. Despite this limitation, this complex can be prepared independently and characterized spectroscopically by ^1H and $^{31}P\{^1H\}$ NMR spectroscopy (vide infra).[31] Treating **1** with *n*-butane (neat or in cyclohexane solution), *n*-pentane, and *n*-hexane cleanly gives rise to the α-olefin complexes, [(PNP)-Ti(η^2-H_2C=$CHCH_2CH_3$)($CH_2{}^tBu$)] (**3**, 1:3 mixture of diastereomers), [(PNP)Ti(η^2-H_2C=CH^nPr)($CH_2{}^tBu$)] (**4**, 1:4 mixture of diastereomers), [(PNP)Ti(η^2-H_2C=CH^nBu)-($CH_2{}^tBu$)] (**5**, 1:4 mixture of diastereomers), respectively (Scheme 3). As opposed to complex **2**, which is unstable at room temperature, complexes **3**−**5** can be isolated as solids that can be stored at −35 °C. These species, however, are not as long-standing as compound **1**, which decomposes only on heating above 65 °C. Lastly, treatment of [(PNP)Ti=$CH^tBu(CH_2{}^tBu)$] with heavier linear alkanes such as *n*-heptane and *n*-octane afforded the longer olefin adducts [(PNP)Ti(η^2-H_2C=CH^nPentyl)($CH_2{}^tBu$)] (**6**, 1:3 mixture of diastereomers) and [(PNP)Ti(η^2-H_2C=CH^nHexyl)($CH_2{}^tBu$)] (**7**, 1:4 mixture of diastereomers),[31] respectively (Scheme 2). Unfortunately, like **2**, these compounds are unstable and decompose within hours (compound **6**) or even minutes (compound **7**) to a myriad of titanium products, along with the corresponding free α-olefin: 1-heptene or 1-octene, respectively.

Complexes **1**−**5** can be independently prepared via salt metathesis reaction of [(PNP)Ti=CH^tBu(OTf)] in Et_2O with the corresponding alkylating reagents $LiCH_2CH_2R$ (R = H, CH_3, CH_2CH_3, ^{n}Pr,[29,32] ^{n}Bu) as shown in Scheme 3, therefore suggesting that formation of these species most likely traverses through the alkylidene-alkyl intermediate, [(PNP)Ti=CH^tBu-(CH_2CH_2R)]. Noteworthy, compound **2** is unstable even by this synthetic method, for which reason complete NMR spectroscopic assignment was not possible (vide infra). Complex **2** is too unstable to explore its reactivity, but in the case of **6** and **7**, we resorted to exposing these systems to ethylene to promote olefin exchange and also to form the more stable ethylene species, **1**. In fact, attempts to prepare **2** from [(PNP)Ti=CH^tBu(OTf)] and $LiCH_2CH_2CH_3$ (generated in situ from $ICH_2CH_2CH_3$ and Li^tBu),[31,32] at −78 °C, resulted in some formation of the propene complex, although workup could not avoid rapid decomposition. Gratifyingly, treating **6** and **7** with 1 atm of ethylene afforded **1**, along with the corresponding olefins 1-heptene and 1-octene, respectively. We are presently unsure of why complex **2** is unstable (or whether an impurity is promoting its decomposition), but in the case of **6** and **7**, the bulkier (or more flexible) group on the olefin may be kinetically destabilizing such species. However, we have found theoretically that formation of the allyl containing complex [(PNP)Ti(η^3-CH_2CHCH_2)] is significantly exothermic (−17.1 kcal/mol) with respect to the propylene adduct **2**. Therefore, one possible mode for decomposition of the latter complex might be the abstraction of the propylene methyl in **2** to form the allyl ligand and free neopentane. Theoretical studies of [(PNP)Ti(η^3-CH_2CHCH_2)] reveal this species to adopt a square-planar geometry with the triplet ground state lying ~7 kcal/mol below the most stable singlet state, and thus, making its detection difficult by standard NMR spectroscopic techniques.[31]

Previously we reported that complex [(PNP)Ti=CH^tBu-($CH_2{}^tBu$)] decomposes to a myriad of products in C_6H_{12} and

Scheme 3. Dehydrogenation of Propane and Linear C_4−C_8 Alkanes by Transient A as well as Independent Preparation of Complexes 2−7 and Olefin Exchange with Complexes 3−7

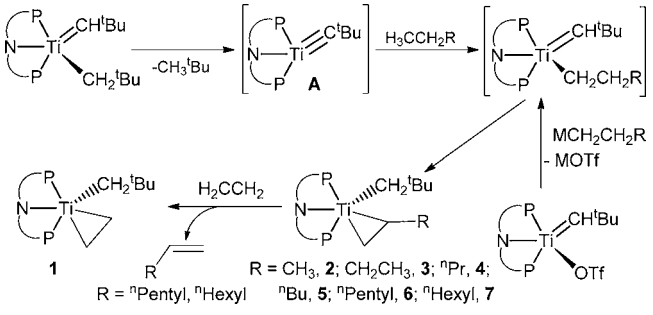

dx.doi.org/10.1021/ja4060178 | J. Am. Chem. Soc. 2013, 135, 14754−14767

that the rate of decay (pseudo-first-order on titanium) was suggestive of **A** being formed in the course of the reaction (k_{avg} = 4.97(2) × 10^{-5} s^{-1}, at 29.6 °C).[27,29] However, when compound [(PNP)Ti=CH^{t}Bu(CH$_2$^{t}Bu)] is allowed to decay in C_6H_{12} over 12 h and the volatiles are examined by GC-MS,[31] we observe formation of cyclohexene exclusively, thus suggesting that **A** must be dehydrogenating the solvent (Scheme 4). We therefore propose that **A** is activating C_6H_{12}

Scheme 4. Proposed Pathway Involving the Dehydrogenation of C_6H_{12} by Transient A and Formation of 1 via the Reaction of Ethylene with Intermediates D or E

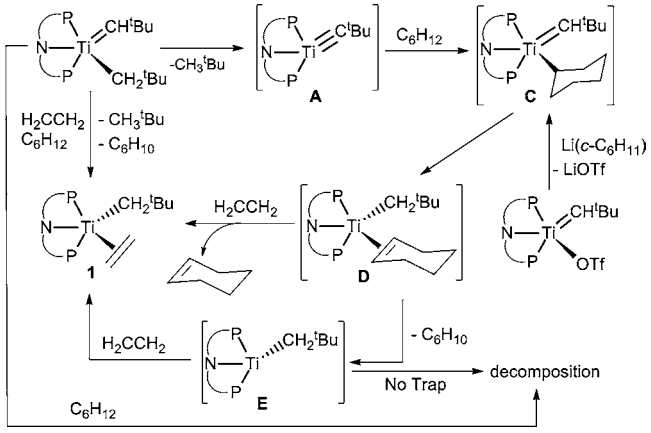

to form a putative cyclohexyl intermediate, [(PNP)Ti=CH^{t}Bu(*c*-C_6H_{11})] (**C**), which then undergoes β-hydrogen abstraction to form the unstable cyclohexene adduct, [(PNP)-Ti(CH$_2$^{t}Bu)(η^2-*c*-C_6H_{10})] (**D**) (Scheme 4). In fact, treating [(PNP)Ti=CH^{t}Bu(OTf)] with Li(*c*-C_6H_{11}) also leads to formation of cyclohexene and innumerable titanium-based products within several hours, as gauged by $^{31}P\{^1H\}$ NMR spectroscopy (Scheme 4). Given that the olefin is sterically crowed (and most likely adopts a chair conformation), intermediate **D** presumably undergoes elimination of cyclohexene to form an unstable titanium(II) species, [(PNP)Ti-(CH$_2$^{t}Bu)] (**E**), which then inexorably decomposes. To test whether a species such as **D** or **E** was likely to form in the aforementioned transformation, we examined the reaction of **1** in C_6H_{12} in the presence of ethylene, since the latter substrate reacts sluggishly with **A** but could rapidly trap the electron-rich putative complex **E**, or exchange with **D**. Indeed, dissolving [(PNP)Ti=CH^{t}Bu(CH$_2$^{t}Bu)] in C_6H_{12} under a headspace of ethylene (1 atm) produced complex **1** along with cyclohexene over 12 h (observed by GC-MS and ^1H NMR spectroscopy).[31] When 1 atm of ethylene is used, some minor decomposition products were observed by $^{31}P\{^1H\}$ NMR spectroscopy, suggesting that ethylene does not entirely trap the titanium(II) species **E** or cleanly exchanges with **D** (Scheme 4). Exposing complex [(PNP)Ti=CH^{t}Bu(CH$_2$^{t}Bu)] to high-pressure ethylene (500 psi) in C_6H_{12} using a reactor vessel[31] still results in some formation of **1** but accompanied by another titanium(IV) complex that has eluded characterization.

Treatment of [(PNP)Ti=CH^{t}Bu(CH$_2$^{t}Bu)] with methylcyclohexane yields methylenecyclohexane as the major product, confirmed by GC-MS analysis of the crude reaction mixture after 12 h. Also, akin to cyclohexane, exposing a methylcyclohexane solution of [(PNP)Ti=CH^{t}Bu(CH$_2$^{t}Bu)] to 1 atm of ethylene forms **1** and the free terminal olefin (Scheme 5).

Scheme 5. Selective Dehydrogenation of Methylcyclohexane and Trapping of the Ti^{2+} Proposed intermediate E with Ethylene To Form 1

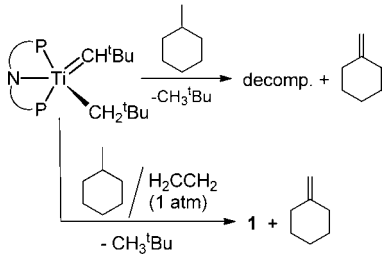

Computational Studies of the Titanium Olefin Complexes. The formation of the titanium olefin complexes **2**–**7** formally follows a mechanism analogous to that of dehydrogenation of ethane to ethylene.[28] As Figure 1 shows for butane, intermediate **A** and free alkane first form a σ-complex (**A-Bu**$_\alpha$) followed by the 1,2-addition of the terminal C–H bond across the reactive Ti≡C linkage (**A-Bu-TS**$_\alpha$) to give rise to the alkyl-neopentylidene intermediate, **B-Bu**$_\alpha$, which finally allows the formation of the dehydrogenated olefin adduct **3** through a concerted metal-mediated β-hydrogen migration step (**B-TS**$_\alpha$). In the cases of long-chain alkanes however, internal C–H bonds are also potentially prone of activation, e.g., leading to β-olefin complexes. Figure 1 clearly reveals why terminal olefin adducts are exclusively observed experimentally: the initial activation of a β-C–H bond of butane is ∼6 kcal mol^{-1} higher in energy than the activation of a terminal C–H bond. Additionally, the olefin adduct **3**$_\beta$ is less stable than **3** by 4.5 kcal mol^{-1}. Moreover, according to our results, **B-Bu**$_\beta$ forms through initial β-C–H activation and inevitably undergoes a subsequent α-C–H cleavage resulting in compound **3**, rather than the γ-bound olefin adduct **3**$_\beta$, a result of the greater stability exhibited by **B-Bu-TS**$_x$ over **B-Bu-TS**$_\beta$. In this light, the study shows that formation of terminal alkenes is both kinetically and thermodynamically more favorable than formation of internal ones in the reaction of **A** with linear alkanes.

We have calculated the structures of compounds **1**–**5** and shown in Figure 2 is that for the parent olefin **1**. Complex **1** adopts a quasi-trigonal bipyramidal geometry with the olefin oriented perpendicular to the equatorial plane (dihedral angles = 7.6°).[31] The simplified Newman projection of this compound (Figure 2) describes the orientation of the olefin as being approximately parallel to the P–Ti–P vector. The latter also indicates clearly how dissymmetry around the titanium center is created as a result of the puckering of the PNP backbone. The C–C distance composing the metallacyclopropane motif is 1.44 Å in **1**, which is significantly elongated to that of free ethylene (1.337(2) Å);[33] comparable to early transition-metal ethylene complexes including Bercaw's (η^5-Cp*)$_2$Ti(η^2-H$_2$C=CH$_2$) (1.438(5) Å),[34] a series of related metallocene derivatives,[35] and Rothwell's (2,6-diphenylphenoxide)$_2$Ti(η^2-H$_2$C=CH$_2$)-(PMe$_3$) (1.425(3) Å)[36,37] ethylene complex (Table 1). Likewise, the computed Ti–$C_{ethylene}$ distances of 2.13 and 2.14 Å are not isometric but are quite similar to the distances observed in structurally characterized titanium ethylene complexes.

dx.doi.org/10.1021/ja4060178 | J. Am. Chem. Soc. 2013, 135, 14754–14767

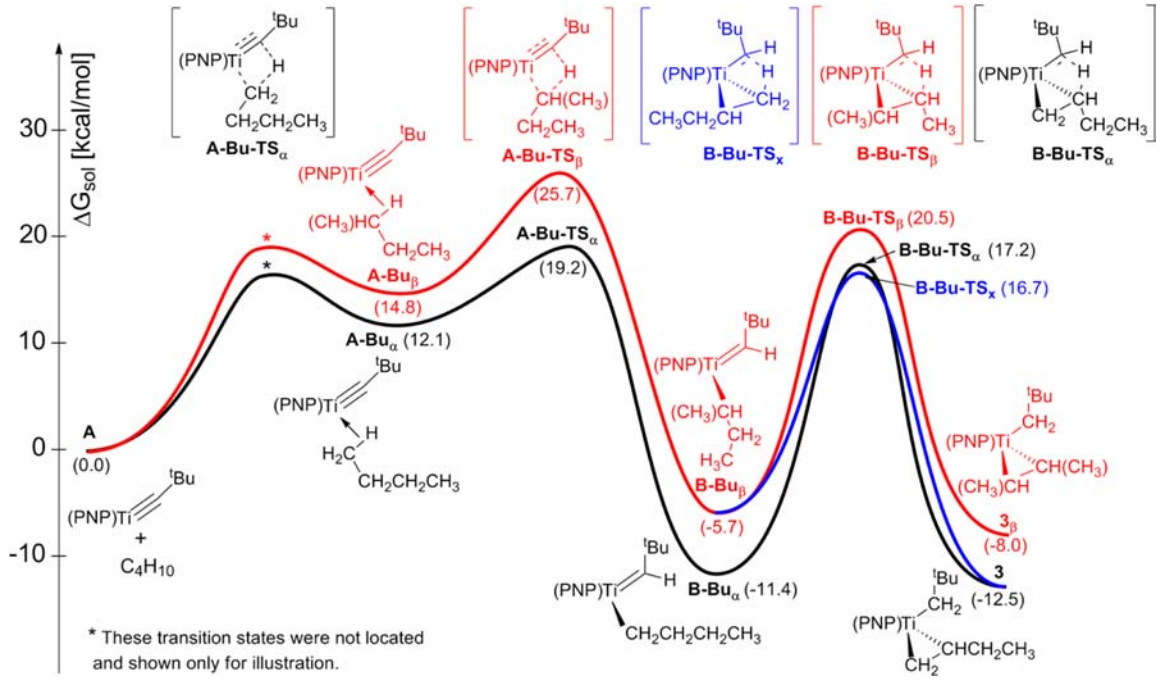

Figure 1. Computed reaction profiles for the dehydrogenation of butane with intermediate **A** leading to terminal and internal olefin complexes. Transition states are shown above the reaction coordinate in brackets.

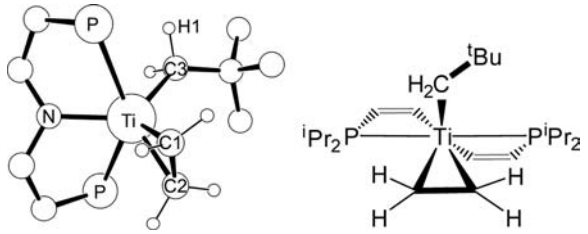

Figure 2. (Left) Optimized geometry of complex **1**. Isopropyl groups and PNP aryl peripherals have been omitted for clarity. (Right) Newman projection of **1** (looking down the Ti−N bond, also with the aryl framework of the PNP backbone omitted for clarity), depicting the orientation of the olefin and pendant neopentyl group in relation to the PNP pincer ligand.

The analysis of the electronic structure of **1** clearly reveals why the investigated titanium olefin product adopts a trigonal bipyramidal geometry with the olefin being parallel to the P−Ti−P vector (Figure 2) and not a quasi-octahedral geometry with C1−C2 perpendicular to the P−Ti−P axis. Figure 3 shows these two plausible arrangements and the relevant metal-olefin interactions assuming C_{2v} symmetry where the d-orbitals transform to b_1 (d_{xz}), a_2 (d_{yz}), a_1 ($d_{x^2-y^2}$), b_2 (d_{xy}) and a_1 (d_{z^2}), as discussed by Burdett and co-workers.[38] Since the electron-donating π-orbital of the ethylene fragment has no orientation selectivity when interacting with the metal d-orbitals, it is only the π^*-orbital that determines the orientation of the olefin with respect to the metal containing fragment. This π^*-orbital can either interact with the low-lying b_1 to make the ethylene fragment align along the axial phosphine ligands ($eq_{\parallel}$, along z, left in Figure 3) or with the b_2 orbital to confine the ethylene perpendicular to the z-axis ($eq_{\perp}$, along y, right in Figure 3). The latter interaction is significantly more advantageous than the former, due to the better energy match of π^* orbital of ethylene with the hybridized d_{xy} + p_y titanium orbitals.[38] Note that in the case of a d^2 metal ion like Ti^{2+}, only b_1 is filled and accordingly, the stabilization of this orbital in the $eq_{\parallel}$ arrangement ($\Delta E_{\parallel}$) is directly manifested in the stabilization of the complex, whereas the $eq_{\perp}$ arrangement is only stabilized by as much as the energy of b_2 dropping below b_1 ($\Delta E_{\perp}$) as a result of the interaction with the π^* of the ethylene. Because of this, the $eq_{\perp}$ type of orientation is more

Table 1. ^{1}H and ^{13}C{^{1}H} NMR Spectroscopic Comparisons of Titanium(η^2-ethylene) Compounds[a]

compound	^{1}H NMR δ (m)	^{13}C{^{1}H} NMR δ (m, $^1J_{CH}$)	C=C (Å)	ref
free ethylene	5.25	122.96 (*s*)	1.337(2)	33
Cp^*_2Ti(ethylene)	2.02 (*s*)	105.1 (*t*, $^1J_{CH}$ = 143.6 Hz)	1.438(5)	34
$(ArO)_2Ti(PMe_3)$(ethylene)	1.72 (*td*), 0.51 (*t*)	78.0 ($^1J_{CH}$ = 147.6 Hz), 67.0 ($^1J_{CH}$ = 149.6 Hz)	1.425(3)	36, 54
$(C_5Me_4SiMe_3)_2Ti$(ethylene)	2.34 (*s*)	104.3 (*s*)	1.442(9)	35a
Cp'_2Ti(ethylene)	2.94 (*s*)	97.8 (*s*)	1.427(5)	35b
$(C_5Me_4{}^tBu)_2Ti$(ethylene)	2.08 (*s*)	101.8 (*s*)	1.454(9)	35c
$(C_5Me_4H)_2Ti$(ethylene)	2.03 (*s*)	102.7 (*s*)	1.446(4)	35c
1	2.3 (*br m*), 1.98 (*br m*), 1.91 (*br m*), 0.93(*br m*)	73.2 ($^1J_{CHa}$ = 153 Hz, $^1J_{CHb}$ = 147 Hz), 67.2 ($^1J_{CHa}$ = 150 Hz, $^1J_{CHb}$ = 150 Hz)	1.44[b]	28 and this work

[a]Cp* = C_5Me_5; ArO = 2,6-diphenylphenoxide; Cp′ = [(1,3-(^{t}Bu)$_2C_5H_3$)], NMR spectroscopic data reported in benzene-d_6. [b]Distance based on DFT calculations.

dx.doi.org/10.1021/ja4060178 | J. Am. Chem. Soc. 2013, 135, 14754−14767

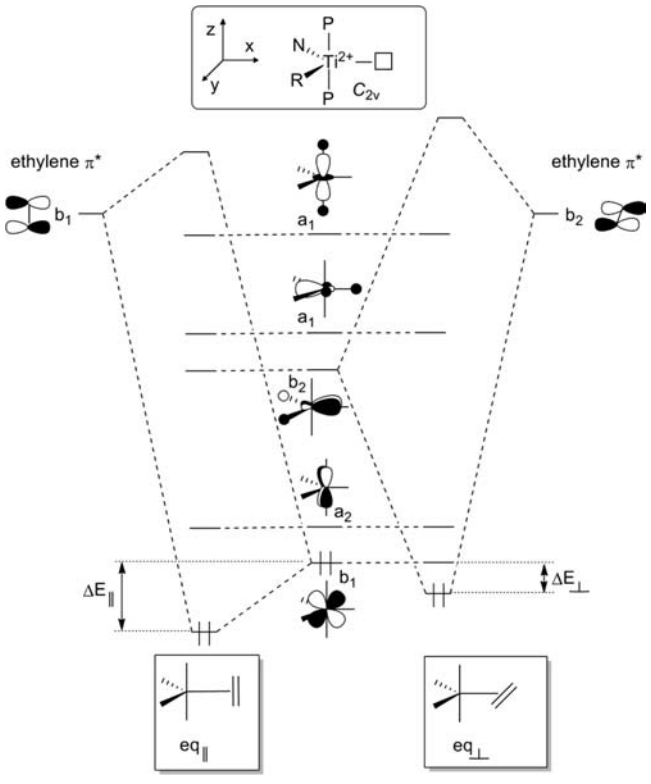

Figure 3. Simplified MO diagram for a π-acceptor ethylene ligand coordinated to the titanium(II) framework (PNP)Ti($CH_2{}^tBu$) in either an $eq_{\parallel}$ or $eq_{\perp}$ fashion.

commonly observed for d^x configurations where $x \geq 6$, because one would then stabilize the populated b_2 orbital as in the case of classical molecule $Fe(CO)_4(\eta^2\text{-}H_2C{=}CH_2)$.[39] Nevertheless, our data clearly converge to the $eq_{\parallel}$ state being 23.7 kcal mol^{-1} *more stable* than the $eq_{\perp}$ state, as indicated in Figure 3.[40,41] Moreover, the $eq_{\perp}$ structure was found to be a transition state corresponding to the rotation of the ethylene fragment, allowing its slow rotation in **1**, at room temperature by traversing a barrier of ~24 kcal mol^{-1}.[31]

In line with computations, in the case of complex **1**, there is no spectroscopic evidence for the formation of isomers even at lower temperatures. However, when propane and linear alkanes C_4–C_8 are dehydrogenated by **A** to form **2**–**7**, two titanium-containing complexes are clearly observed spectroscopically by $^{31}P\{^1H\}$ and $^{13}C\{^1H\}$ NMR (vide infra). For each alkane, we propose these two resulting species to be a mixture of diastereomers which arise from different orientations of the neopentyl ligand and the R group of the olefin relative to the PNP backbone. Since the PNP pincer ligand is akin to C_2-symmetric, chiral phosphine ligands such as DuPhos[42] or BINAP,[43] which are commonly used in asymmetric catalysis, it is not surprising that α-olefin adducts would give rise to stereoisomers. These isomers, having axial chirality,[44] can adopt either R_a or S_a configurations defined by the handedness of the axis that relates them. Scheme 6 shows these orientations for PNP in a five-coordinate complex where the other two equatorial ligands, R^1 and R^2, are inequivalent. The two orientations R_a and S_a shown in Scheme 6 are enantiomers and thus are not discernible by standard NMR spectroscopic techniques. Since there are two orientations of the skewed aryl groups of PNP, along with two possible orientations of the bound olefin (both oriented along the P–Ti–P axis) and two

Scheme 6. Axial Chirality Gives Rise to Four Chemically Inequivalent Positions of the Alkyl Chain (right) for Complexes 2–7, Whereby C^2 is a Stereogenic Center

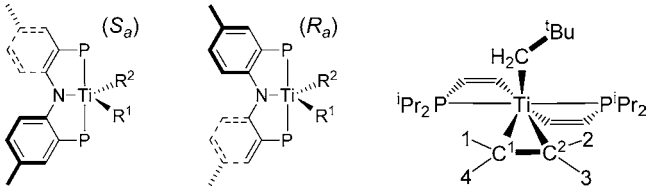

more orientations of the neopentyl group, a total of eight different diastereomers is possible, each with its corresponding enantiomer (16 combinations in total). Scheme 7 depicts the Newman projection for these eight possible diastereomers based on the orientation of the aryl groups (with the aryl backbone removed for clarity), the neopentyl group and the location of R group on the olefin. As a point of reference, the first *syn* or *anti* abbreviation refers to the orientation of the neopentyl group with respect to the olefin, R or S represents the configuration generated by the twisted aryl moieties, while the second *syn* or *anti* abbreviations represent the orientation of the R group of the olefin with respect to the neopentyl ligand.

To scrutinize the effect of R and how this affects the energy of the conformers we calculated the solvent phase free energies of the possible isomers with various substituents (R = H, CH_3, CH_2CH_3, ^{n}Pr, ^{n}Bu, ^{n}Pentyl).[31] The relative free energies of the various conformers as a function of R, respective to **A** and free alkane, are given in Figure 4. Note that although the energy difference between structures is only a few tenths of kcal mol^{-1} in some cases (which is beyond the error of our computational protocol), a few chemically meaningful trends can be inferred from Figure 4. For example, it is easy to observe that shifting from ethylene to longer alkenes, the olefin complex becomes less stable by about 5 kcal mol^{-1}. Also, in the case of **1** (R = H), the energy difference between the *syn* and *anti* isomers, denoting the orientation of the neopentyl group with respect to the olefin (*syn*-**1** versus *anti*-**1**) is about 2 kcal mol^{-1}, preferring the *syn* arrangement. This difference diminishes if the R group of the olefin also points into the *syn* position. Both of these trends can be explained by the steric repulsion of the bulky alkyl groups on the PNP and the bound olefins, the effects of which are greater with increasing length of the R group on the latter, i.e., going from ethylene to longer alkenes, the R group collides with the ^{i}Pr groups of the PNP backbone resulting in an overall destabilization of the complexes. Moreover, whenever the neopentyl substituent and the R group of the olefin occupy the *syn* positions (*syn*-R-*syn* or *syn*-S-*syn*), they clash into each other, further abating their stability.

Only three stable isomers were calculated for R = ^{n}Bu and ^{n}Pentyl, due to the high computational demand of these structures. However, the trend observed for these species fits nicely with that of shorter alkenes. Thus, based on the relative energies of the conformers, we propose that the experimentally detected two-product species most likely correspond to the *syn*-R-*anti* and *anti*-S-*syn* arrangements. Then again, it is easy to judge why the R group of the olefin, the bulky ^{i}Pr groups of the PNP backbone, and the neopentyl substituent elicit the most advantageous arrangements in these two isomers, minimizing the overall steric repulsion and resulting in the more stable structures. It is also important to note that the relationship of the conformers is probably even more complex than illustrated here, since interconversion might take place via the rotation of

dx.doi.org/10.1021/ja4060178 | J. Am. Chem. Soc. 2013, 135, 14754–14767

Scheme 7. Computed Diastereomers for the α-Olefin Complexes of Titanium Where R = CH_3, CH_2CH_3, ^{n}Pr, ^{n}Bu, ^{n}Pentyl

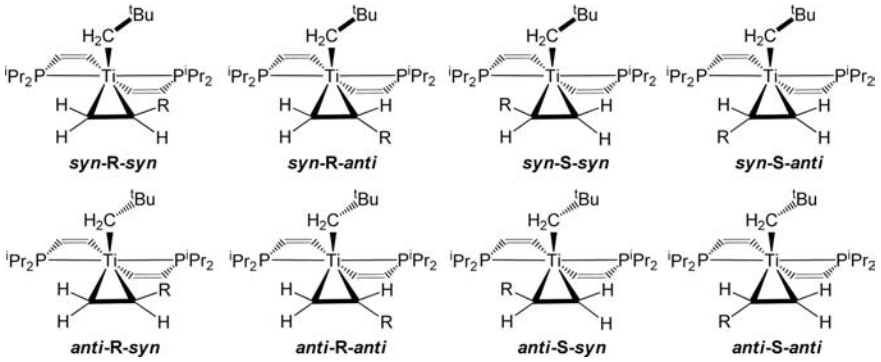

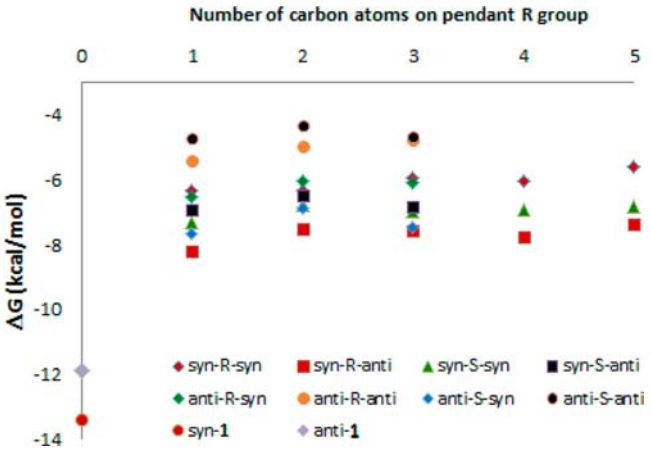

Figure 4. Relative stabilities (ΔG_{sol}) of the possible conformers of the olefin complexes [(PNP)Ti(η^2-H_2C═CHR)($CH_2{}^tBu$)], in kcal mol^{-1}, as a function of the R group (H, CH_3, CH_2CH_3, ^{n}Pr, ^{n}Bu, ^{n}Pentyl). Stabilities are given respective to **A** and free alkane.

the olefin fragment. Such rotation has been calculated to have an activation barrier of about 20−23 kcal mol^{-1} with R = CH_3 and CH_2CH_3, depending on the position of the R group.

NMR Spectroscopic Characterization of the Titanium Olefin Complexes. The $^{31}P\{^1H\}$ NMR spectrum of complex **1** exhibits two doublets at 28.06 and 26.05 ppm with $^2J_{PP}$ = 22.2 Hz (Figure S5), while the ^1H NMR spectrum, along with the selective- and fully decoupled $^1H\{^{31}P\}$ NMR, and $^1H-^{31}P$ HMBC spectra (Figures S6−S12) clearly assigns the two diastereotopic methylene protons for the neopentyl fragment at 1.28 (d, $^2J_{HH}$ = 11.5 Hz) and 0.021 ppm (dt, $^2J_{HH}$ = 12.0, $^3J_{HP}$ = 2.6 Hz). Of these, the more shielded resonance exhibits coupling to both the geminal proton and the two phosphorus atoms in the PNP backbone giving rise to a doublet of triplets, whereas the deshielded resonance at 1.28 ppm exhibits solely geminal proton coupling and resolves only into a doublet, albeit overlapping with the isopropyl-methyl resonances of the PNP. The fact that complex **1** could not be obtained as single crystals led us to fully investigate its structural features in solution with the aid of numerous NMR spectroscopic experiments. In addition to 1D (^1H, $^1H\{^{31}P\}$, $^{13}C\{^1H\}$) NMR spectra, the complete connectivity of **1** was elucidated by a battery of state-of-the-art 2D NMR techniques including double quantum filtered (dqf) COSY, DEPT-135, and C−H coupled/C−H decoupled gradient $^1H-^{13}C$ HSQC experiments. Each hydrogen in the ethylene unit of complex **1** is inequivalent (^1H NMR: 2.3, 1.98, 1.91, 0.93 ppm) and should thus be diastereotopic. Unfortunately these resonances are broad and featureless in the ^1H NMR spectrum and are often difficult to assign due to overlap with isopropyl resonances from the PNP. Gratifyingly, the dqfCOSY spectrum (Figure 5, left) clearly discerns the

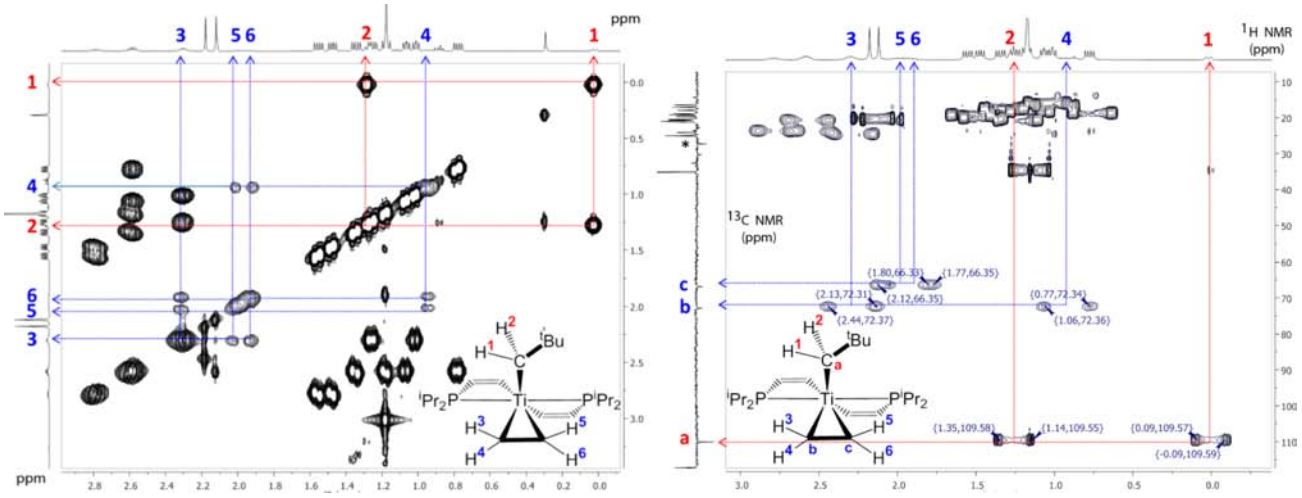

Figure 5. Expanded absolute-phase dqfCOSY (left) and C−H coupled $^1H-^{13}C$ gHSQC (right) NMR spectra of complex **1**. Numeric assignments of the olefin hydrogen or carbons are arbitrary. Spectra have been cropped (the large ^{t}Bu resonance in the ^1H NMR has been cropped). *Represents residual solvent in the spectrum. Numbers in parentheses for the right spectrum represent chemical shifts for the ^1H and ^{13}C spectra.

dx.doi.org/10.1021/ja4060178 | J. Am. Chem. Soc. 2013, 135, 14754−14767

Table 2. Summarized Key NMR Spectroscopic Data for Olefin Compounds 1−7

	^{1}H				^{13}C{^{1}H}			^{31}P{^{1}H}	
	TiCH_aH_b^{t}Bu		Ti(CH_2=CH-R)		Ti-CH_aH_b^{t}Bu	Ti(CH_2=CH-R)		(P_1NP_2)Ti	
	δ_1 (m, $^2J_{HH}$)^b TiCH_aH_b^{t}Bu	δ_2 (m, $^2J_{HH}$, $^3J_{HP}$)^b TiCH_aH_b^{t}Bu	δ_1 (m), δ_2 (m) Ti(CH_2CH-R)	δ_3 (m) Ti(CH$_2$CH-R)	δ ($^1J_{CHa}$, $^1J_{CHb}$)^c Ti-CH_aH_b^{t}Bu	δ_1 ($^1J_{CHa}$, $^1J_{CHb}$)^c Ti(CH_2CH-R)	δ_2 ($^1J_{CHa}$, $^1J_{CHb}$)^c Ti(CH$_2$CH-R)	δ_1 (m, $^2J_{PP}$)^b (P_1NP$_2$)Ti	δ_2 (m, $^2J_{PP}$)^d (P$_1$NP_2)Ti
1 (R = H)	1.28 (d, 11.5Hz)	0.021 (dt, 12Hz, 2.6Hz)	2.3 (m), 0.93 (m)	1.98 (m), 1.91 (m)	110.37 (101Hz, 97Hz)	73.2 (153Hz, 147Hz)	67.2 (150Hz, 150Hz)	28.06 (d, 22.2Hz)	26.05 (d, 22.2Hz)
2 (R = Me)^a	1.55 (dd, 12 Hz, 2Hz)	0.68 (d, 12 Hz)	1.58 (m) 0.95 (m)	1.78 (m)	--	--	--	26.71 (d, 22.2Hz)	21.03 (d, 22.2Hz)
3 (R = Et)	1.5 (m)	0.59 (dt, 11.6Hz, 2.8Hz)	1.69 (m), 1.18 (m)	1.76 (m)	109.8 (106Hz, 99Hz)	78.9 (143Hz, 150Hz)	86.8 (134 Hz)	27.06 (d, 21Hz)	21.14 (d, 21Hz)
4 (R = ^{n}Pr)	1.49 (m)	0.645 (dt, 11.5Hz, 2Hz)	1.69 (m), 1.19 (m)	1.79 (m)	109.6 (105Hz,101Hz)	79.8 (146Hz, 148Hz)	84.1 (147 Hz)	26.9 (d, 21.1Hz)	20.52 (d, 21.1Hz)
5 (R = ^{n}Bu)	1.51 (m)	0.665 (dt, 12Hz, 2Hz)	1.67 (m), 1.25 (m)	1.79 (m)	109.3 (107Hz,101Hz)	79.7 (146Hz, 152Hz)	84.5 (139 Hz)	27.05 (d, 21.2Hz)	20.67 (d, 21.2Hz)
6 (R = ^{n}Pentyl)^a	--	--	--	--	--	--	--	26.58 (d, 21.4Hz)	20.28 (d, 21.4Hz)
7 (R = ^{n}Hex)^a	--	--	--	--	--	--	--	26.69 (d, 21.4Hz)	20.36 (d, 21.4Hz)

^{a}Compound decomposes very rapidly. No ^{13}C{^{1}H} NMR could be recorded. ^{b}$^2J_{HH}$ and $^3J_{HP}$ measured from the ^{1}H NMR spectra. ^{c}$^1J_{CH}$ values measured from C−H coupled ^{1}H−^{13}C gHSQC experiments. ^{d}Only chemical shifts of the major diastereomer are listed.

cross-correlation resonances that arise from the three spin systems: the correlation between the diasterotopic protons in the Ti-CH$_2$^{t}Bu moiety and the cross-peaks due to the resonances of the four protons in the ethylene ligand of **1**. As with the diastereotopic protons on Ti-CH_2^{t}Bu (red trace), the protons on the bound ethylene fragment are nonfluxional and also diastereotopic (blue trace), with each of these protons giving individual resonances which is consistent with the olefinic carbons being locked in a distorted geometry around titanium (Figure 5, left). The C−H decoupled ^{1}H−^{13}C gHSQC spectrum of **1** further corroborates the above conclusion with the individual resonances for the diastereotopic protons on the methylene carbons appearing clearly resolved (Figure S15). However, some of the most informative NMR spectroscopic data were extracted from a C−H coupled ^{1}H−^{13}C gHSQC experiment (Figure 5, right). In addition to being able to clearly assign the CH$_2$ groups in the ^{13}C-DEPT trace (shown as negative resonances), this experiment allowed us to precisely extract the magnitudes of the $^1J_{CH}$ coupling constants for the Ti-CH_2^{t}Bu (~99 Hz) and the H_2C=CH_2 (~150 Hz) moieties on complex **1** (Tables 1 and 2). Noteworthy, the magnitudes of the coupling constants of the diastereotopic methylene protons on Ti-CH_2^{t}Bu are unusually small respective to typical $^1J_{CH}$ values of unpolarized alkane bonds, H-CHRR′ (R = H, Me; R′ = Me), which range from ~119 to 125 Hz, whereas the $^1J_{CH}$ values of the bound H_2C=CH_2 are only slightly smaller from the ones reported for free ethylene (156.2 Hz).[33a] The low $^1J_{CH}$ value for the neopentyl-methylene protons is a strong evidence of a large electropositive character inflicted by the titanium center, with the magnitude of these constants being comparable to that observed in methyllithium ($^1J_{CH}$ = 98 Hz).[45] The fact that the values of the $^1J_{CH}$ constants of the ethylene moiety in **1** are affected to a much lesser extent by the titanium center tantalizingly implies little distortion of the s-character on the sp^2 hybridized carbons of the bound olefin, which could in turn suggest weak back-donation to form a metallacyclopropane resonance, **1a** (Scheme 2, vide supra). Comparison of the ^{1}H and ^{13}C{^{1}H} NMR spectroscopic data and crystallographic parameters for the few known titanium-ethylene complexes are listed in Table 1.

Lastly, we wanted to gather information regarding the spatial orientation of the neopentyl and ethylene fragments with respect to the phosphines of the PNP ligand. Accordingly, we collected a ^{1}H−^{31}P HOESY spectrum of **1** (Figure 6), which

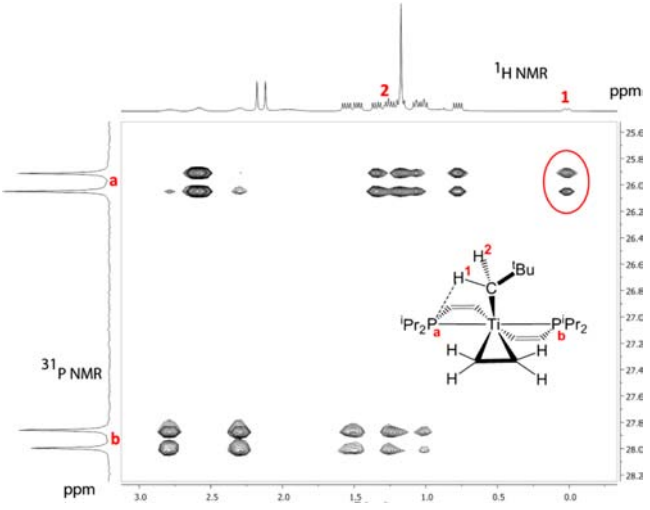

Figure 6. Expansion of the ^{1}H−^{31}P HOESY (400 MHz, 25 °C) spectrum of complex **1**, highlighting in a red circle the spatial correlation between the more shielded resonance of the Ti-CH$_2$^{t}Bu moiety (0.02 ppm) and the PNP-phosphorus resonance at 26.05 ppm. A dotted line in the scheme indicates our rationale for this spatial correlation.

revealed that the more shielded diastereotopic proton on the Ti−CH_2^{t}Bu ligand (0.02 ppm) clearly correlates through space to only one phosphorus resonance at 26.05 ppm. This result suggests that the corresponding proton is somewhat aligned with one phosphorus and/or points in that direction. Conversely, the fact that the other methylene proton in Ti-CH$_2$^{t}Bu gives no tangible correlation to either phosphorus

dx.doi.org/10.1021/ja4060178 | J. Am. Chem. Soc. 2013, 135, 14754−14767

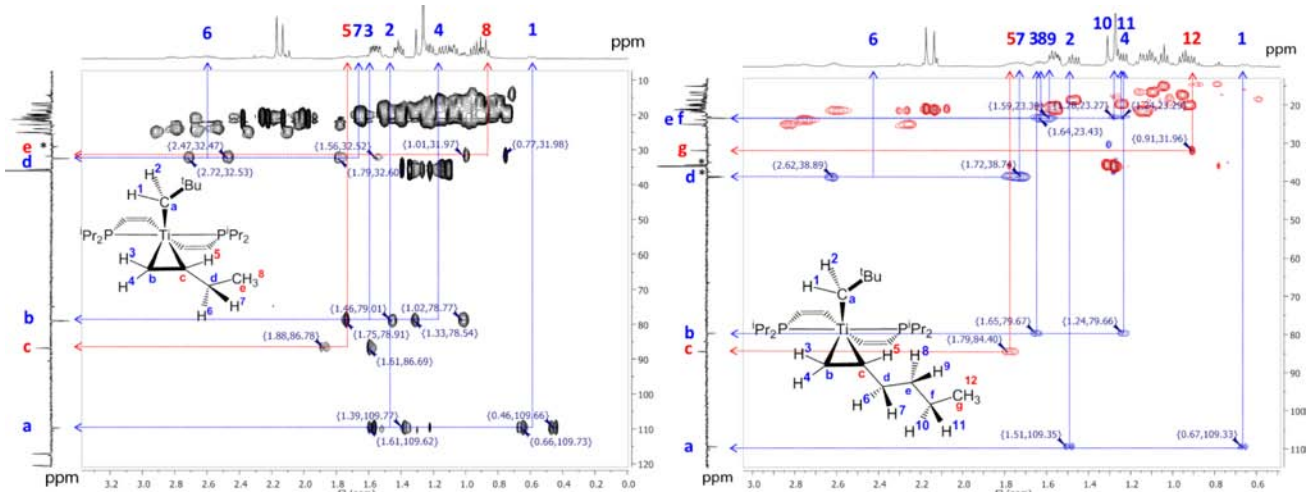

Figure 7. Expanded C−H coupled $^{1}H-^{13}C$ gHSQC NMR spectrum of complex **3** (left). Right is the C−H decoupled gHSQC NMR spectrum of complex **5**. Spectra have been cropped (the large ^{t}Bu resonance in the ^{1}H NMR spectrum has been cropped). *Represents residual solvent. Numbers in parentheses represent chemical shifts for the ^{1}H and ^{13}C spectra.

resonance suggests that it is locked in a geometrical conformation pointing away from both phosphorus atoms. As a result, it is quite possible that the neopentyl group in **1** is not oriented strictly in the forward position or that the P−Ti−P angle is highly distorted due to the Ti−P distances not being isometric and far from a transoid orientation. From the ^{1}H, $^{13}C\{^{1}H\}$, and $^{13}P\{^{1}H\}$ NMR spectroscopic data it can be generalized that all hydrogens on the ethylene ligand are shielded when compared to free ethylene. In addition, $^{1}J_{CH}$ values fall in the 143−153 Hz range. Overall, NMR spectroscopic data of Rothwell's complex $(ArO)_2Ti(\eta^2\text{-}H_2C{=}CH_2)(PMe_3)$ (ArO^- = 2,6-diphenylphenoxide)[36,37] are similar to that observed for **1**, presumably due to these systems being more electronically unsaturated. Salient ^{1}H and $^{13}C\{^{1}H\}$ NMR spectroscopic data for complex **1** are included in Table 2.

Since complex **2** is unstable in solution over several hours, we provide only 1D ^{1}H and $^{31}P\{^{1}H\}$ NMR spectra (Table 2). For this reason, we focus our attention on complexes **3**−**5** since these systems are much more stable and should not significantly differ from **2**. The NMR spectroscopic characterization of the α-olefin complexes **3**−**5** follows a similar trend to that for **1**, with the exception that the two isomers can be observed by both $^{31}P\{^{1}H\}$ and $^{13}C\{^{1}H\}$ NMR spectroscopy. The ^{1}H NMR spectra do not reveal the presence of isomers, suggesting these to have coincidental chemical shifts (as in the case of **2**). Compound **2** can only be observed spectroscopically as a mixture of two isomers by $^{31}P\{^{1}H\}$ NMR due to rapid decomposition (Table 2). However, complexes **3**−**5** are relatively stable and have been unambiguously established by solution NMR spectroscopy. Table 2 reports the most important spectroscopic features for all these species, including the longer and more unstable olefins **6** and **7**. For comparative purposes we will focus our attention on complex **3**.

The $^{31}P\{^{1}H\}$ NMR spectrum of complex **3** clearly reveals a ratio of two diastereomers of ∼5:1 with the major diastereomer exhibiting resonances at 27.1 (d, $^{2}J_{PP}$ = 21 Hz) and 21.1 ppm (d, $^{2}J_{PP}$ = 21 Hz). The minor diastereomer is observed at 26.64 (d, $^{2}J_{PP}$ = 22.2 Hz) and 24.82 ppm (d, $^{2}J_{PP}$ = 22.2 Hz). The relative ratio of these two species does not change upon heating (>50 °C) of the solution, and this is also the case with all the higher olefin adducts (**4** and **5**). This indicates that the diastereomers are not interconverting with each other (at least not in the temperature range tested). Akin to **1**, the ^{1}H NMR spectrum of **3** reveals a shielded doublet of triplets at 0.59 ppm ($^{2}J_{HH}$ = 11.6, $^{3}J_{HP}$ = 2.8 Hz), consistent with a diastereotopic methylenic proton that is simultaneously coupled to both phosphorus atoms in the PNP backbone and the other geminal proton in the Ti-$CH_2{}^{t}Bu$ moiety. Unlike **1** however, the chemical shift of the latter resonance is considerably obscured by peak overlap with the PNP ligand and the aliphatic moiety of the bound olefin.[31]

We relied on C−H decoupled and coupled (Figure 7) $^{1}H-^{13}C$ gHSQC spectra to fully assign the connectivity around the titanium centers as well as accurately measure the $^{1}J_{CH}$ coupling constants derived from the Ti-$CH_2{}^{t}Bu$ and $Ti(\eta^2\text{-}H_2C{=}CHCH_2CH_3)$ core fragments and the pendant aliphatic chain, $Ti(\eta^2\text{-}H_2C{=}CHCH_2CH_3)$. These $^{1}J_{C-H}$ coupling constants are listed in Table 2. In Figure 7 (left) it can be observed how the protons on all CH_2 moieties of **3** are diastereotopic. The contours for the methylene protons on Ti-$CH_2{}^{t}Bu$ appear as distinct blue, negative contours, at virtually the same chemical shifts as the ones observed in compound **1**. The methylene carbon exhibits a resonance at ∼110 ppm (C−H decoupled $^{1}H-^{13}C$ gHSQC; Figure 7, left). In addition, the negative contours derived from the protons on the $Ti(\eta^2\text{-}H_2C{=}CHCH_2CH_3)$ moiety are aligned with the carbon resonance of this fragment at 78.9 ppm, similar to the respective one associated to $Ti(\eta^2\text{-}H_2C{=}CH_2)$ in **1**, at 73 ppm. Unlike **1**, the contour for the vinylic C−H proton in $Ti(\eta^2\text{-}H_2C{=}CHCH_2CH_3)$ is considerably deshielded with its carbon resonance located as a positive peak at 86.7 ppm on the DEPT-135 trace shown in red (labeled 5) in Figure 7, left. Such unique pattern is also observed for the longer α-olefin adducts, **4** and **5** (Figures S34 and S46). In terms of the magnitude of the $^{1}J_{CH}$ coupling constant on the Ti-$CH_2{}^{t}Bu$ and $Ti(\eta^2\text{-}H_2C{=}CHCH_2CH_3)$ core fragments in **3**, these values are in exact line with the ones determined for such fragment in compound **1** (Table 2). Notably, the $^{1}J_{CH}$ constant for the allylic CH group has a slightly smaller magnitude of 134 Hz, likely indicative of a more polarized fragment. The magnitudes for the diastereotopic methylene protons in the $-CH_2CH_3$ substituent of the bound butene in **3** are all within normal values for sp^3

dx.doi.org/10.1021/ja4060178 | J. Am. Chem. Soc. 2013, 135, 14754−14767

Table 3. Summary of Alkane Dehydrogenation Kinetics

entry	substrate	T (°C)	conv. (%)	$k \times 10^{-5}$ (s^{-1})[a]	$\sigma \times 10^{-5}$	$t_{1/2}$ (h)	KIE[b]
1	pentane	29.7	90	6.0	0.5	3.2	1.1
2	pentane-d_{12}	29.8	90	5.6	0.5	3.5	
3	hexane	29.7	83	5.48	0.01	3.5	
4	pentane:hexane (1:1)	29.6	79	5.115	0.005	3.8	
5	heptane	29.65	82	5.0	0.6	3.9	
6	octane	29.7	74	4.0	0.7	4.9	
7	cyclohexane	29.6	89	4.97	0.02	3.9	1.2
8	cyclohexane-d_{12}	28.9	88	4.2	0.1	4.6	
9	methylcyclohexane	29.7	84	5.0	0.2	3.9	
10	1-hexene	29.9	88	5.7	0.4	3.4	

[a]All reactions were performed in duplicates. [b]KIE = k_H/k_D

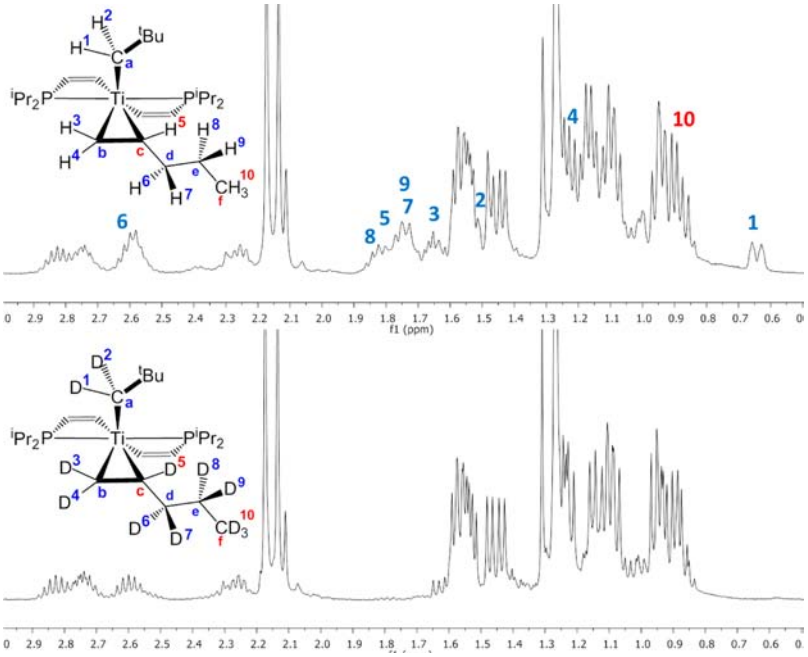

Figure 8. Overlaid expansions of the ^{1}H NMR spectra (400 MHz, 25 °C) of the partially deuterated (bottom) and fully protiated (top) pentene adducts **4**-d_{12} and **4**, respectively.

hybridized carbons and in the range of 118 to 122 Hz. In this context, the fact that the bound olefin exhibits both stereogenic carbon centers and distinct values for the $^1J_{CH}$ coupling constants for the allylic groups in $H_2C{=}CHCH_2CH_3$ is indicative of a highly rigid metallacyclopropane moiety as proposed for resonance **1a** with considerably greater degree of covalency between the titanium center and the olefin. As the alkyl chain becomes longer, the chemical shifts of the more distal methylene groups become essentially equivalent in the ^{1}H NMR spectrum, hence no longer being diastereotopic. In fact, the diastereotopic character of the methylenic protons on the bound α-olefin decreases sharply after the δ-carbon, with the protons of this and the ε-carbon of the hexene adduct **5** already displaying nearly single-type contours indicative of their equivalence (Figure 7, right). The C−H decoupled and coupled ^{1}H−^{13}C gHSQC spectra for **4** and **5** clearly portray these subtle differences as a function of alkyl chain growth (Figures S33, S34, S45, and S46). The ^{13}C{^{1}H} NMR spectra of **3**−**5** in the ^{1}H−^{13}C gHSQC experiment clearly show the other diastereomer present in solution (what appear as small impurities next to each ^{13}C resonance), and the DEPT trace reveals this species to contain the same set of vinylic and allylic groups in addition to the neopentyl ligand. In Figure 7 (right), the C−H decoupled ^{1}H−^{13}C gHSQC NMR spectrum of complex **5** exposes the analogous pattern to complex **3** for hydrogens numbered 1−5, the olefinic carbons b and c, and the allylic carbon d. Likewise, the minor diastereomer is also observed in the vertical DEPT-135 NMR trace.

Mechanistic Studies Involving the Dehydrogenation of Alkanes by Transient A. Complex [(PNP)Ti=CH^{t}Bu-($CH_2{}^t$Bu)] decays cleanly in neat solutions of *n*-pentane, *n*-hexane, *n*-heptane, and *n*-octane with nearly identical rates (Table 3). These pseudo-first-order decay rates are very similar to those measured for reactions with benzene ($6.5(4) \times 10^{-5}$ s^{-1} at 27 °C),[27] methane (7.9×10^{-5} s^{-1} at 31 °C, 1150 psi),[10c] and cyclohexane (5.86×10^{-5} s^{-1} at 31 °C).[10c] Therefore, formation of intermediate **A** is most likely the slowest step in the conversion of alkanes C_2−C_8 to the corresponding titanium olefin adducts. In fact, the rates for decay of [(PNP)Ti=CH^{t}Bu($CH_2{}^t$Bu)] are similar in cyclohexane versus methylcyclohexane, and mixtures of alkanes (hexane/pentane) did not result in unequal formation of the olefin complexes. To test if other steps such as 1,2-CH bond addition or β-hydrogen abstraction were competitive with α-hydrogen abstraction in

dx.doi.org/10.1021/ja4060178 | J. Am. Chem. Soc. 2013, 135, 14754−14767

[(PNP)Ti=CH^{t}Bu(CH$_2$^{t}Bu)] to **A**, we examined the rate of decay of this precursor in pentane-d_{12} and found that the KIE was close to unity (1.1 at ~29 °C, Table 3).[31] In addition, ^{1}H and ^{2}H NMR spectra confirm formation of the isotopologue [(PNP)Ti(η^2-D$_2$C=CDCD$_2$CD$_2$CD$_3$)(CD$_2$^{t}Bu)] (**4**-d_{12}), where complete deuteration of the alkylidyne carbon in transient **A** has occurred. Figure 8 depicts the ^{1}H NMR spectrum of **4** overlaid with **4**-d_{12} thus showing full deuteration of the neopentyl (labels 1 and 2 in blue) and olefin residues (labels for the methylenes 3, 4, and 6–9 (all in blue) as well as the vinylic 5 (red) and terminal CH$_3$, 10, in red). This result indicates that transfer of the hydrogens must be occurring at the alkylidyne moiety of **A**. In a sense, the conversion of an alkane to the olefin in our system involves an intramolecular transfer dehydrogenation pathway, whereby the alkylidyne ligand is the hydrogen acceptor.

Exposure of **4**-d_{12} to 1 atm of ethylene (slight excess) slowly formed [(PNP)Ti(η^2-H$_2$C=CH$_2$)(CD$_2$^{t}Bu)] (**1**-d_2) and the terminal olefin, 1-pentene-d_{10}.[46] Likewise, addition of ethylene to a solution of [(PNP)Ti=CH^{t}Bu(CH$_2$^{t}Bu)] in C$_6$D$_{12}$ also formed **1**-d_2 and C$_6$D$_{10}$. Comparison of the rates of decay (pseudo-first order) of **1** in C$_6$H$_{12}$ versus C$_6$D$_{12}$ yielded a KIE of 1.2 at 29 °C (Table 3). Therefore, all our data suggest that [(PNP)Ti=CH^{t}Bu(CH$_2$^{t}Bu)] forms **A** slowly, while 1,2-CH bond addition of the alkane to form the alkylidene-alkyl, [(PNP)Ti=CH^{t}Bu(CH$_2$CHR)], as well as β-hydrogen abstraction to form the olefin-bound diastereomers, [(PNP)Ti(η^2-H$_2$C=CHR)(CH$_2$^{t}Bu)], are all post-rate determining steps.

To establish whether complex **1** liberates the olefin, we treated this compound with a slight excess of D$_2$C=CD$_2$ (1 atm) in C$_6$H$_6$ or C$_6$D$_6$. Over 72 h at 25 °C, complex **1** does exchange with D$_2$C=CD$_2$ to form [(PNP)Ti(η^2-D$_2$C=CD$_2$)(CH$_2$^{t}Bu)] (**1**-d_4) and free H$_2$C=CH$_2$ but does so not cleanly giving the formation of another titanium product which we have been unable to characterize. In addition, we also see slow incorporation of deuterium in the neopentyl ligand, thus implying that β-hydrogen abstraction might be a reversible process and that **1** and intermediate **B** could equilibrate slowly (Scheme 8). Because the reaction between **1** and D$_2$C=CD$_2$ is not clean, we cannot exclude other processes by which the deuterium becomes incorporated in the neopentyl ligand of **1**, such as α-elimination[47] in **E** to form an alkylidene-hydride (PNP)Ti=CH^{t}Bu(H) followed by migratory insertion of ethylene to form **B** (Figure 8). Rothwell reported reversible homo coupling of ethylene with (ArO)$_2$Ti(η^2-H$_2$C=CH$_2$)(PMe$_3$) to form the metallacyclopentane species (ArO)$_2$Ti(H$_2$CCH$_2$CH$_2$CH$_2$).[36,37] For our case, we propose olefin exchange in **1** to occur via a dissociative mechanism and theoretical studies suggest the S = 1 intermediate **E** to be only 4.6 kcal/mol higher in energy than the ethylene adduct. The results of this study have been published elsewhere.[29]

Scheme 8. Exchange of Ethylene-d_4 with 1 via Dissociation of Ethylene and Tautomerization or by α-Elimination and Insertion of the Olefin

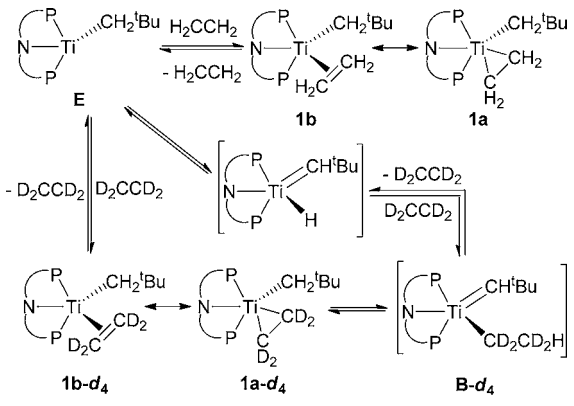

Two-Electron Oxidation Reactions of the Titanium Olefin Complexes. Although **1** and **3**–**7** can sluggishly extrude the olefin above 50 °C, no titanium product(s) could be isolated. For this reason, we explored two-electron oxidants that could promote not only elimination of the olefin but also form a stable titanium byproduct. Based on studies by Bergman and Andersen involving the reactivity of (η^5-Cp*)$_2$Ti(η^2-C$_2$H$_4$) with various oxidants to form Ti=NR,[48] Ti=O,[49] Ti=CR$_2$,[50] and Ti=S[51] functionalities and free ethylene, we decided to explore similar reactivity with our titanium olefin complexes. These reactions would also provide an indirect method to characterize the olefin moiety as well as the site of dehydrogenation in the case of compounds **3**–**7**. As noted previously,[28] exposing **1** to a bed of N$_2$O in C$_6$H$_6$ or C$_6$D$_6$ immediately lead to a color change from brown to wine-red, concurrent with formation of [(PNP)Ti=O(CH$_2$^{t}Bu)] (**8**) and free ethylene (Scheme 9). As shown in Scheme 9,

Scheme 9. Oxidation of 1 with N$_2$O, N$_3$R (R = 1-adamantyl or SiMe$_3$), 2 OCPh$_2$, and N$_2$Ctolyl$_2$[a]

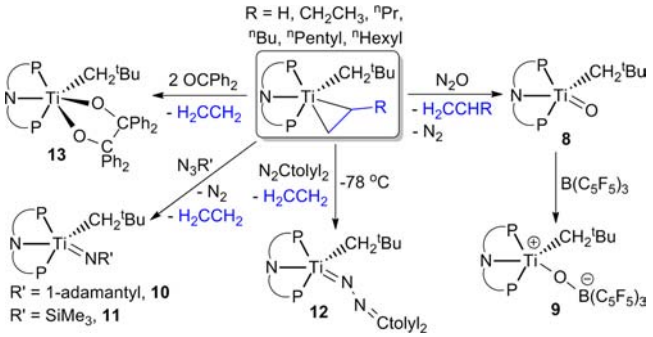

[a]Oxidation of **3**–**7** with N$_2$O to release the terminal olefin are also illustrated.

compound **8** has been previously reported and is unstable over several hours in solution, at room temperature. However, complex **8** can be trapped with B(C$_6$F$_5$)$_3$ to form the stable zwitterion [(PNP)Ti{OB(C$_6$F$_5$)$_3$}(CH$_2$^{t}Bu)] (**9**) (Scheme 9), which has been characterized by ^{1}H and ^{31}P{^{1}H} NMR spectroscopy, in addition to a solid-state crystal structure.[31,40,52] Treating **1** with N$_3$R′ also leads to ethylene formation along with the stable titanium imidos [(PNP)Ti=NR′(CH$_2$^{t}Bu)] (R′ = 1-adamantyl, **10**; SiMe$_3$, **11**). Compounds **8**, **10**, and **11** have been structurally characterized and were discussed in an earlier communication.[28] Likewise, addition of N$_2$Ctolyl$_2$ at low temperatures (−110 °C) leads to clean formation of the diazoalkane [(PNP)Ti=NNCtolyl$_2$(CH$_2$^{t}Bu)] (**12**) in 74% yield, along with free ethylene (Scheme 9). The reaction must be performed at low temperature, otherwise N$_2$Ctolyl$_2$ further reacts with **12** to give other titanium species which will be omitted from this discussion. Unlike metallocene-diazoalkane complexes,[51,53] complex **12** does not extrude N$_2$ to form alkylidene intermediates, nor do we have any spectroscopic

dx.doi.org/10.1021/ja4060178 | J. Am. Chem. Soc. 2013, 135, 14754–14767

evidence for the N_2Ctolyl$_2$ ligand engaging in a side-on fashion with the titanium center. For example, the chemical shift of one diastereotopic TiCH_2^{t}Bu proton, δ = 1.36 ppm, does not shift downfield as it does with another titanium species having side-on ligands.[31] To more accurately compare the reactivity of **1** with other titanium ethylene complexes, we turned our attention to benzophenone since this substrate is known to produce 3-, 5-, and even 7-metallacycles.[37] Accordingly, exposure of **1** with 1 equiv of benzophenone results in 50% formation of complex (PNP)Ti(CH_2^{t}Bu)(TPP) (**13**) (TPP^{2-} = tetraphenylpinacolato) and ethylene along with titanium starting material, as a consequence of coupling of two benzophenone molecules. In addition to NMR spectroscopic data, the connectivity of **13** was elucidated by X-ray diffraction (using a poorly diffracting single crystal), confirming the formation of the pinacolato framework.[31,40,54] Addition of 2 equiv of the ketone forms **13** in better yield (~80% isolated yield, Scheme 9). The reactivity of **1** toward benzophenone differs completely from Rothwell's (ArO)$_2$Ti(η^2-H_2C=CH_2)(PMe_3) complex with two equiv of $OCPh_2$ to release PMe_3 and form a seven-membered ring in (ArO)$_2$Ti($OCPh_2CH_2CH_2CPh_2O$).[37] Unlike Cp*$_2$Ti(η^2-H_2C=CH_2) or (ArO)$_2$Ti(η^2-H_2C=CH_2)(PMe_3), which do not release free ethylene in solution, the mechanism leading to formation of compounds **8**−**13** might not involve an insertion pathway. This is especially true since compound **1** slowly releases ethylene and is more coordinatively saturated. However, the possibility of insertion chemistry involving the ethylene ligand in **1** cannot be ruled out since the labile phosphine arms in PNP could be dissociating in these reactions.

We also explored the reactivity of the α-olefin complexes **3**−**7**. In all cases, addition of a 1 atm of N_2O to these compounds elicited rapid formation of complex **8** and corresponding free olefin (Scheme 9). Only formation of the linear, terminal olefin C_4−C_8 was observed based on ^{1}H NMR spectroscopy and GC-MS. Reactions with N_2O are quantitative and cleaner than olefin exchange reactions with ethylene (vide supra), Scheme 3.

CONCLUSIONS

In this work we have studied the reactivity of transient **A** with the volatile alkanes C_2−C_8. In all cases dehydrogenation takes place to afford species of the type [(PNP)Ti(η^2-H_2C=CHR)(CH_2^{t}Bu)] (R = H, CH_3, CH_2CH_3, ^{n}Pr, ^{n}Bu, ^{n}Pentyl, and ^{n}Hexyl). When C_4−C_8 alkanes are dehydrogenated, only the α-olefins are observed. The ethylene complex is the most stable form, and in the case of R = Me, ^{n}Pentyl, and ^{n}Hexyl, the olefin adducts are too unstable to fully characterize. The dehydrogenation of alkanes by **A** takes place through a two-step mechanism starting with a 1,2-addition of the terminal C−H bond to the Ti≡C functionality followed by a metal-mediated β-hydrogen migration. DFT studies have revealed that the exclusive formation of α-olefins has kinetic and thermodynamic origins. A combination of theory and multidimensional spectroscopic data suggests the olefin in [(PNP)Ti(η^2-H_2C=CHR)(CH_2^{t}Bu)] to be oriented along the P−Ti−P vector, where the neopentyl group points opposite the aryl groups of the PNP ligand. This characteristic feature was rationalized within the MO framework with the interaction of the π* of the olefin with the corresponding metal d-orbitals. A product distribution was proposed based on the relative stabilities of the possible conformers. Compound [(PNP)Ti(η^2-H_2C=CHR)(CH_2^{t}Bu)] can extrude the olefin under thermolytic conditions, but release of the olefin is much cleaner when these complexes are exposed to oxidants such N_2O, N_3R, and N_2Ctolyl$_2$. Complex [(PNP)Ti(η^2-H_2C=CH_2)(CH_2^{t}Bu)] also reacts with two equiv of benzophenone to afford the pinacol coupled product, concomitant with release of ethylene. Cyclohexane and methylcyclohexane can be also dehydrogenated by **A**, at room temperature, to cyclohexene and methylenecyclohexane respectively, and the putative Ti(II) species formed from decoordination of the olefin can be trapped with ethylene. Kinetic and isotopic labeling studies suggest the dehydrogenation steps not to be the rate-determining while reactions using D_2C=CD_2 reveal exchange of the olefin in [(PNP)Ti(η^2-H_2C=CH_2)(CH_2^{t}Bu)], in addition to a scrambling phenomenon involving the olefin and the α-hydrogens of the neopentyl group. The fact that the alkylidyne precursor [(PNP)Ti=CH^{t}Bu(CH_2^{t}Bu)] reacts sluggishly with ethylene suggests that dehydrogenation of the alkane to olefin is preferred over dehydrogenation of an alkene to an alkyne or activation of the more thermodynamically vulnerable allylic C−H bonds. Preliminary studies have revealed that when [(PNP)Ti=CH^{t}Bu(CH_2^{t}Bu)] is treated with 1-hexene for 12 h, followed by quenching of the reaction with N_2O, some formation of 1,5-hexadiene is observed in addition to some other hydrocarbon products.[31] This result, although premature, suggests that **A** is somewhat selective toward the dehydrogenation of alkanes and that a linear alkane can be converted, stepwise and stoichiometrically, to the corresponding terminal diene. This transformation holds great promise since one could envision the direct conversion of a hydrocarbon such as butane to butadiene or transforming a branched alkane such as 2-methylbutane to isoprene. Both of these dienes are heavily used in the production of synthetic or natural rubber, respectively.

ASSOCIATED CONTENT

Supporting Information

X-ray crystallographic information (CIF), isotopic and kinetic studies, kinetic analysis, spectral data, reactions, and computational studies. This material is available free of charge via the Internet at http://pubs.acs.org.

AUTHOR INFORMATION

Corresponding Author

mindiola@indiana.edu and mindiola@sas.upenn.edu

Present Address

[†]Department of Chemistry, University of Pennsylvania, 231 South 34th Street, Philadelphia, Pennsylvania 19104-6323.

Notes

The authors declare no competing financial interest.

ACKNOWLEDGMENTS

Financial support of this research was provided by the National Science Foundation (CHE-0848248 and CHE-1152123). M.G.C. acknowledges CONACYT for a postdoctoral fellowship. The authors thank Prof. Allen Siedle and Prof. Mu-Hyun Baik for insightful discussions. J.-I.I. acknowledges financial support from the JSPS (Japan Society for the Promotion of Science).

REFERENCES

(1) (a) Walsh, B. *Time* **2012**, *179* (14), 28. (b) Johnson, J.; Scott, A. *Chem. Eng. News* **2013**, *91*, 12. (February 18, 2013) (c) Scott, A. *Chem. Eng. News* **2013**, *91*, 16. (February 18, 2013) (d) Johnson, J. *Chem. Eng. News* **2013**, *91*, 22 (February 18, 2013).

(2) (a) In *Viewing America's Energy Future in Three Dimensions*, Hegedus, L. L.; Temple, D. S., Eds.; RTI Press : Research Triangle Park, NC, 2011. (b) Ground Water Protection Council; ALL Consulting. Modern Shale Gas Development In The United States: A Primer, U.S. Department of Energy, Office of Fossil Energy and National Energy Technology Laboratory, April 2009 [cited 2010 Aug 28]. Available from: http://www.netl.doe.gov/technologies/oil-gas/publications/EPreports/Shale_Gas_Primer_2009.pdf. (c) Speight, J. G. In *Kirk-Othmer Encyclopedia of Chemical Technology*, 4th ed., Kroschwitz, J. I., Howe-Grant, M., Eds.; John Wiley & Sons: New York, 1993, Vol. *12*, pp 126−155. (d) Han, S.; Chang, C. D. In *Kirk-Othmer Encyclopedia of Chemical Technology*, 4th ed., Kroschwitz, J. I., Howe-Grant, M., Eds.; John Wiley & Sons: New York, 1993, Vol. *12*, pp 155−203.

(3) (a) Johnson, J.; Tullo, A. H. *Chem. Eng. News* **2013**, *91*, 9. (b) Tullo, A. H. *Chem. Eng. News* **2013**, *91*, 6. (c) Johnson, J. *Chem. Eng. News* **2013**, *91*, 18. (d) Johnson, J. *Chem. Eng. News* **2012**, *90*, 30. (e) Reisch, M. S. *Chem. Eng. News* **2012**, *90*, 12. (f) Johnson, J. *Chem. Eng. News* **2012**, *90*, 30. (g) Bomgardner, M. M. *Chem. Eng. News* **2012**, *90*, 13. (h) Tullo, A. H. *Chem. Eng. News* **2012**, *90*, 6. (i) Tullo, A. H. *Chem. Eng. News* **2012**, *90*, 10. (j) Tullo, A. H. *Chem. Eng. News* **2011**, *89*, 26. (k) Tullo, A. H. *Chem. Eng. News* **2011**, *89*, 22. (l) Tullo, A. H. *Chem. Eng. News* **2009**, *87*, 26. (m) Johnson, J. *Chem. Eng. News* **2005**, *83*, 19.

(4) Gold, R. Firms Plan to Export Gas. In *The Wall Street Journal*, January 25, **2011**.

(5) The controlled C−H activation of aliphatic bonds has been described as a "Holy Grail" in Chemistry, see: (a) Bard, A. J.; Whitesides, G. M.; Zare, R. N.; McLafferty, F. W. *Acc. Chem. Res.* **1995**, *28*, 91. (b) Arndtsen, B. A.; Bergman, R. G.; Mobley, T. A.; Peterson, T. H. *Acc. Chem. Res.* **1995**, *28*, 154. (c) For the first use this phrase in a research oriented manuscript. Lippard, S. J. *Acc. Chem. Res.* **1978**, *11*, 211−217.

(6) For relevant examples of catalytic functionalization of alkanes, including direct functionalization of methane to methanol: (a) Hashiguchi, B. G.; Bischof, S. M.; Konnick, M. M.; Periana, R. A. *Acc. Chem. Res.* **2012**, *45*, 885. (b) Copéret, C. *Chem. Rev.* **2010**, *110*, 656. (c) Hartwig, J. F. *Nature* **2008**, *455*, 314. (d) Sorokin, A. B.; Kudrik, E. V.; Bouchu, D. *Chem. Commun.* **2008**, 2562. (e) Bar-Nahum, I.; Khenkin, A. M.; Neumann, R. *J. Am. Chem. Soc.* **2004**, *126*, 10236. (f) Kakiuchi, F.; Chatani, N. *Adv. Synth. Catal.* **2003**, *345*, 1077. (g) Chen, H. Y.; Schlecht, S.; Semple, T. C.; Hartwig, J. F. *Science* **2000**, *287*, 1995. (h) Periana, R. A.; Taube, D. J.; Gamble, S.; Taube, H.; Satoh, T.; Fujii, H. *Science* **1998**, *280*, 560. (i) Periana, R. A.; Taube, D. J.; Evitt, E. R.; Loffler, D. G.; Wentrcek, P. R.; Voss, G.; Masuda, T. *Science* **1993**, *259*, 340.

(7) For select reviews on homogeneous alkane C−H activation: (a) In *Catalysis by Metal Complexes*; Pérez, P. J., Ed.; Springer: New York, 2012, Vol. *38* (Alkane C−H Activation by Single-Site Metal Catalysis), pp 1−264. (b) Basset, J.-M.; Copéret, C.; Soulivong, D.; Taoufik, M.; Thivolle Cazat, J. *Acc. Chem. Res.* **2010**, *43*, 323. (c) Balcells, D.; Clot, E.; Eisenstein, O. *Chem. Rev.* **2010**, *110*, 749. (d) West, N. M.; Templeton, J. L. *Can. J. Chem.* **2009**, *87*, 288. (e) Bercaw, J. E.; Labinger, J. A. *Proc. Natl. Acad. Sci. U.S.A.* **2007**, *104*, 6899. (f) Pombeiro, A. J. L. *ACS Symp. Ser.*, **2007**, Vol. *974* (Vanadium), pp. 51−60. (g) Periana, R. A.; Bhalla, G.; Tenn, W. J., III; Young, K. J. H.; Liu, X. Y.; Mironov, O.; Jones, C. J.; Ziatdinov, V. R. *J. Mol. Catal. A: Chem.* **2004**, *220*, 7. (h) Schreiner, P. R.; Fokin, A. A. *Chem. Rec.* **2004**, *3*, 247. (i) Cui, W. H.; Wayland, B. B. *J. Am. Chem. Soc.* **2004**, *126*, 8266. (j) Crabtree, R. H. *J. Organomet. Chem.* **2004**, *689*, 4083. (k) Fokin, A. A.; Schreiner, P. R. *Adv. Synth. Catal.* **2003**, *345*, 1035. (l) Jones, W. D. *Acc. Chem. Res.* **2003**, *36*, 140. (m) Labinger, J. A.; Bercaw, J. E. *Nature* **2002**, *417*, 507. (n) Crabtree, R. H. *J. Chem. Soc., Dalton Trans.* **2001**, *17*, 2437. (o) Eisenstein, O.; Crabtree, R. H. *New J. Chem.* **2001**, *25*, 665. (p) Stahl, S. S.; Labinger, J. A.; Bercaw, J. E. *Angew. Chem., Int. Ed.* **1998**, *37*, 2180. (q) Shilov, A. E.; Shul'pin, G. B. *Chem. Rev.* **1997**, *97*, 2879. (r) Vidal, V.; Théolier, A.; Thivolle-Cazat, J.; Basset, J.-M. *Science* **1997**, *276*, 99. (s) Crabtree, R. H. *Chem. Rev.* **1995**, *95*, 987. (t) Crabtree, R. H. *Chem. Rev.* **1985**, *85*, 245. (u) Bergman, R. G. *Science* **1984**, *223*, 902. For a recent critical review on homogeneous alkane dehydrogenation by transition metals. (v) Dobereiner, G. E.; Crabtree, R. H. *Chem. Rev.* **2010**, *110*, 681.

(8) Recent reviews on homogeneous C−H activation of alkanes using iridium compounds: (a) Haibach, M. C.; Kundu, S.; Brookhart, M.; Goldman, A. S. *Acc. Chem. Res.* **2012**, *45*, 947. (b) Crabtree, R. H. *Top. Organomet. Chem.* **2011**, *34*, 1. (Iridium Catalysis) (c) Jongwook, C.; Goldman, A. S. *Top. Organomet. Chem.* **2011**, *34*, 139. (Iridium Catalysis) (d) Morales-Morales, D. In *Iridium Complexes in Organic Synthesis*, Oro, L. A.; Claver, C., Eds.; Wiley-VCH: New York, 2009, 325. (e) Goldman, A. S.; Ghosh, R. In *Handbook of C-H Transformations - Applications in Organic Synthesis*, Dyker, G., Ed.; Wiley-VCH: New York, 2005, 616. (f) Goldman, A. S.; Goldberg, K. I. *ACS Symp. Ser.* 2004, *885*, 1. (g) Krogh-Jespersen, K.; Czerw, M.; Goldman, A. S. *J. Mol. Catal. A: Chem.* **2002**, *189*, 95. (h) Fan, H.-J.; Hall, M. B. *J. Mol. Catal. A: Chem.* **2002**, *189*, 111. (i) Maguire, J. A.; Boese, W. T.; Goldman, M. E.; Goldman, A. S. *Coord. Chem. Rev.* **1990**, *97*, 179.

(9) (a) Zhu, Q.; Wegener, S. L.; Xie, C.; Uche, O.; Neurock, M.; Marks, T. J. *Nat. Chem.* **2013**, *5*, 104. (b) Flores, J. A.; Cavaliere, V. N.; Buck, D.; Pintér, B.; Chen, G.; Crestani, M. G.; Baik, M.-H.; Mindiola, D. J. *Chem. Sci.* **2011**, *2*, 1457. (c) Hashiguchi, B. G.; Hoevelmann, C. H.; Bischof, S. M.; Lokare, K. S.; Leung, C. H.; Periana, R. A. In *Methane to Methanol Conversion. Energy Production and Storage: Inorganic Chemical Strategies for a Warming World*; Crabtree, R. H., Ed.; Wiley: New York, 2010, 101. (d) Palkovits, R.; Antonietti, M.; Kuhn, P.; Thomas, A.; Schüth, F. *Angew. Chem., Int. Ed.* **2009**, *48*, 6909. (e) Holmen, A. *Catal. Today* **2009**, *142*, 2. (f) Chen, G. S.; Labinger, J. A.; Bercaw, J. E. *Proc. Natl. Acad. Sci. U.S.A.* **2007**, *104*, 6915. (g) Lunsford, J. H. *Catal. Today* **2000**, *63*, 165. (h) Lunsford, J. H. *Catal. Today* **1990**, *6*, 235. (i) Baerns, M.; van der Wiele, K.; Ross, J. R. H. *Catal. Today* **1989**, *4*, 471.

(10) (a) Cavaliere, V. N.; Mindiola, D. J. *Chem. Sci.* **2012**, *3*, 3356. (b) Cavaliere, V. N.; Wicker, B. F.; Mindiola, D. J. *Adv. Organomet. Chem.* **2012**, *60*, 1. (c) Flores, J. A.; Cavaliere, V. N.; Buck, D.; Chen, G.; Crestani, M. G.; Pinter, B.; Baik, M.-H.; Mindiola, D. J. *Chem. Sci.* **2011**, *2*, 1457−1462.

(11) Hiller, H.; et al. In *Ullman's Encyclopedia of Industrial Chemistry*, 6th ed.; Bohnet, M., et al., Eds.; Wiley-VCH: Weinheim, Germany, 2003, Vol. *15*, pp 305−470.

(12) (a) Pässler, P. In *Ullman's Encyclopedia of Industrial Chemistry*, 6th ed.; Bohnet, M., et al., Eds.; Wiley-VCH: Weinheim, Germany, 2003, Vol. *1*, pp 248−249. (b) Obenaus, F.; Droste, W.; Neumeister, J. In *Ullman's Encyclopedia of Industrial Chemistry*, 6th ed.; Bohnet, M., et al., Eds.; Wiley-VCH, Weinheim, Germany, 2003, Vol. *16*, pp 4−6. (c) Griesbaum, K.; et al. In *Ullman's Encyclopedia of Industrial Chemistry*, 6th ed.; Bohnet, M., et al., Eds.; Wiley-VCH: Weinheim, Germany, 2003, Vol. *17*, pp 4−7. (d) Calamur, N.; Carrera, M. E.; Wilsak, R. A. In *Kirk-Othmer Encyclopedia of Chemical Technology*, 4th ed.; Kroschwitz, J. I., Howe-Grant, M., Eds.; John Wiley & Sons, New York, 1993, Vol. *4*, pp 711−715.

(13) Some select monographs and reviews: (a) Maitlis, P. M.; de Klerk, A. Eds.; In *Greener Fischer−Tropsch Processes for Fuels and Feedstocks*, Wiley-VCH: Weinheim, Germany, 2013, pp 1−363. (b) Baliban, R. C.; Elia, J. A.; Floudas, C. A. *AIChE J.* **2013**, *59*, 505. (c) West, N. M.; Miller, A. J. M.; Labinger, J. A.; Bercaw, J. E. *Coord. Chem. Rev.* **2011**, *255*, 881. (d) Storch, H. H.; Golumbic, N.; Anderson, R. B. *In The Fischer−Tropsch and Related Syntheses*, John Wiley & Sons: New York, 1951, pp 1−610. For specific overviews of coal liquefaction, pertinent to the Fischer−Tropsch synthesis: (e) Kaneko, T.; Derbyshire, F.; Makino, E.; Gray, D.; Tamura, M. In *Ullman's Encyclopedia of Industrial Chemistry*, 6th ed.; Bohnet, M., et al., Eds.; Wiley-VCH, Weinheim, Germany, 2003, Vol. *8*, pp 635−717. (f) Baldwin, R. M. In *Kirk-Othmer Encyclopedia of Chemical Technology*, 4th ed., Kroschwitz, J. I., Howe-Grant, M. Eds.; John Wiley & Sons: New York, USA, 1993, Vol. *6*, pp 568−594.

(14) Jacoby, M. *Chem. Eng. News* **2006**, *84*, 57.

(15) Tullo, A. H. *Chem. Eng. News* **2011**, *89*, 20.

(16) Tullo, A. H. *Chem. Eng. News* **2007**, *85*, 27.
(17) Galvis, H. M. T.; Bitter, J. H.; Khare, C. B.; Ruitenbeek, M.; Dugulan, A. I.; de Jong, K. P. *Science* **2012**, *335*, 835.
(18) Xu, W.-w.; Rosini, G. P.; Krogh-Jespersen, K.; Goldman, A. S.; Gupta, M.; Jensen, C. M.; Kaska, W. C. *Chem. Commun.* **1997**, 2273.
(19) Goldman, A. S.; Roy, A. H.; Huang, Z.; Ahuja, R.; Schinski, W.; Brookhart, M. *Science* **2006**, *312*, 257.
(20) Cobar, E. A.; Khaliullin, R. Z.; Bergman, R. G.; Head-Gordon, M. *Proc. Natl. Acad. Sci. U.S.A.* **2007**, *104*, 6963.
(21) Nomura, K.; Saito, Y. *J. Chem. Soc., Chem. Commun.* **1988**, 161−162. (c) Nomura, K.; Saito, Y. *J. Mol. Catal.* **1989**, *54*, 57−64. (d) Sakakura, T.; Sodeyama, T.; Tanaka, M. *New J. Chem.* **1989**, *13*, 737−745. (e) Sakakura, T.; Sodeyama, T.; Abe, F.; Tanaka, M. *Chem. Lett.* **1991**, 297−298.
(22) Gruver, B. C.; Adams, J. J.; Warner, S. J.; Arulsamy, N.; Roddick, D. M. *Organometallics* **2011**, *30*, 5133−5140.
(23) (a) Gupta, M.; Hagen, C.; Flesher, R. J.; Kaska, W. C.; Jensen, C. M. *Chem. Commun.* **1996**, 2083. (b) Gupta, M.; Hagen, C.; Kaska, W. C.; Cramer, R. E.; Jensen, C. M. *J. Am. Chem. Soc.* **1997**, *119*, 840. (c) Haenel, M. W.; Oevers, S.; Angermund, K.; Kaska, W. C.; Fan, H. J.; Hall, M. B. *Angew. Chem., Int. Ed.* **2001**, *40*, 3596.
(24) (a) Belli, J.; Jensen, C. M. *Organometallics* **1996**, *15*, 1532. (b) Mediati, M.; Tachibana, G. N.; Jensen, C. M. *Inorg. Chem.* **1992**, *31*, 1827.
(25) Ahuja, R.; Punji, B.; Findlater, M.; Supplee, C.; Schinski, W.; Brookhart, M.; Goldman, A. S. *Nature Chem.* **2011**, *3*, 167−171.
(26) Biswas, S.; Huang, Z.; Choliy, Y.; Wang, D. Y.; Brookhart, M.; Krogh-Jespersen, K.; Goldman, A. S. *J. Am. Chem. Soc.* **2012**, *134*, 13276−13295.
(27) (a) Bailey, B. C.; Fan, H.; Huffman, J. C.; Baik, M.-H.; Mindiola, D. J. *J. Am. Chem. Soc.* **2007**, *129*, 8781. (b) Mindiola, D. J. *Acc. Chem. Res.* **2006**, *39*, 813. (c) Bailey, B. C.; Fan, H.; Baum, E. W.; Huffman, J. C.; Baik, M.-H.; Mindiola, D. J. *J. Am. Chem. Soc.* **2005**, *127*, 16016.
(28) Cavaliere, V. N.; Crestani, M. G.; Pinter, B.; Pink, M.; Chen, C.-H.; Baik, M.-H.; Mindiola, D. J. *J. Am. Chem. Soc.* **2011**, *133*, 10700.
(29) Crestani, M. G.; Pinter, B.; Olasz, A.; Bailey, B. C.; Fortier, S.; Gao, X.; Chen, C.-H.; Baik, M.-H.; Mindiola, D. J. *Chem. Sci.* **2013**, *4*, 2543−2550.
(30) (a) Dewar, M. J. S. *Bull. Soc. Chim. Fr.* **1951**, C79. (b) Chatt, J.; Duncanson, L. A. *J. Chem. Soc.* **1953**, 2929.
(31) See Supporting Information.
(32) *n*-Propyllithium solid was synthesized via addition of 2 equiv of 1.7 M ^{t}BuLi (7 mL, 0.0118 mol) to 0.9995 g (0.0059 mol) of iodopropane in ether at −78 °C. The solution was stirred for 1 h and then taken to dryness in vacuo. Pentane was then added to the solid. The solution was allowed to stir, followed by decanting of the pentane to remove impurities. After drying in vacuo, 0.9012 g of white powdery solid was recovered. Coordination of two ether molecules is evident in the ^{1}H NMR spectrum.
(33) (a) Fulmer, G. R.; Miller, A. J. M.; Sherden, N. H.; Gottlieb, H. E.; Nudelman, A.; Stoltz, B. M.; Bercaw, J. E.; Goldberg, K. I. *Organometallics* **2010**, *29*, 2176−2179. (b) Thompson. *Trans. Faraday Soc.* **1939**, *35*, 697. (c) Keesom; Toconis. *Physica* **1935**, *2*, 463. (d) Bartell, L. S.; Roth, E. A.; Hollowell, C. D.; Kuchitzu, K.; Young, J. E. *J. Chem. Phys.* **1965**, *42*, 2683.
(34) Cohen, S. A.; Auburn, P. R.; Bercaw, J. E. *J. Am. Chem. Soc.* **1983**, *105*, 1136−1143.
(35) For other examples of titanocene-ethene adducts. (a) Horáček, M.; Kupfer, V.; Thewalt, U.; Štěpnička, P.; Polášek, M.; Mach, K. *Organometallics* **1999**, *18*, 3572−3578. (b) Walter, M. D.; Sofield, C. D.; Andersen, R. A. *Organometallics* **2008**, *27*, 2959−2970. (c) Pinkas, J.; Císařová, I.; Gyepes, R.; Kubišta, J.; Horáček, M.; Mach, K. *Organometallics* **2012**, *31*, 5478−5493.
(36) Thorn, M. G.; Hill, J. E.; Waratuke, S. A.; Johnson, E. S.; Fanwick, P. E.; Rothwell, I. P. *J. Am. Chem. Soc.* **1997**, *119*, 8630.
(37) Hill, J. E.; Fanwick, P. E.; Rothwell, I. P. *Organometallics* **1992**, *11*, 1771.
(38) (a) Albright, T. A.; Burdett, J. K.; Whangbo, M. H. In *Orbital Interactions in Chemistry*; Wiley: New York, 1985. The bonding and rotation of five-coordinate ethylene complexes have been also discussed in a paper. (b) Albright, T. A.; Hoffmann, R.; Thibeault, J. C.; Thorn, D. L. *J. Am. Chem. Soc.* **1979**, *101*, 3801−3812.
(39) (a) Davis, M. I.; Speed, C. S. *J. Organomet. Chem.* **1970**, *21*, 401−413. (b) Ittel, S. D.; Ibers, J. A. *Adv. Organomet. Chem.* **1976**, *14*, 33−61.
(40) Cavaliere, V. N. M.Sc. Thesis, Department of Chemistry, Indiana University, Bloomington, IN, 2012.
(41) The orientation of the ethene moiety has been confirmed by an X-ray structure of the oxide dimer $[(PNP)Ti(\eta^2\text{-}C_2H_4)]2(\mu^2\text{-}O)$: monoclinic, *C*2/*c*, T = 150(2) K, a = 15.338(3) Å, b = 18.091(3) Å, c = 24.184(4) Å, $\alpha = \gamma = 90°$, β = 95.050°, Z =4, V = 6684.7(19) Å^3, absorption coefficient = 0.375 mm^{-1}, $F(000)$ = 2536, R_{int} = 0.1759; a total of 44 836 reflections collected in the range $1.69° < \theta < 27.62°$, of which 7720 were unique. GOF = 0.799, R_1 = 0.516 and wR_2 = 0.0942 (for all data), largest diff. peak and hole = 0.410/−0.275. See Supporting Information for full crystallograhic characterization (ref 31).
(42) Burk, M. J. *J. Am. Chem. Soc.* **1991**, *113*, 8518.
(43) Noyori, R.; Ohta, M.; Hsiao, Y.; Kitamura, M.; Ohta, T.; Takaya, H. *J. Am. Chem. Soc.* **1986**, *108*, 7117.
(44) Christie, G. H.; Kenner, J. *J. Chem. Soc., Trans.* **1922**, *121*, 614.
(45) McKeever, L. D.; Waack, R.; Doran, M. A.; Baker, E. B. *J. Am. Chem. Soc.* **1969**, *91*, 1057−1061.
(46) Attempts to cleanly generate the isotopologue $[(PNP)Ti(\eta^2\text{-}H_2CCH_2)(CD_2{}^{t}Bu)]$ (**1**)-d_2 by treatment of **4**-d_{12} with 1 atm of ethylene resulted in formation of more than one product. Formation of the isotopologue **1**-d_2 is observed but overtime there is incorporation of proton in the neopentyl group.
(47) (a) Fellmann, J. D.; Tuner, H. W.; Schrock, R. R. *J. Am. Chem. Soc.* **1980**, *102*, 6608−6609. (b) Antonelli, D. W.; Schaefer, W. P.; Parkin, G.; John, E.; Bercaw, J. E. *J. Organomet. Chem.* **1993**, *462*, 213−220. (c) Van Asselt, A.; Burger, B. J.; Gibson, V. C.; Bercaw, J. E. *J. Am. Chem. Soc.* **1986**, *108*, 5347−5349. (d) Schrock, R. R.; Seidel, S. W.; Mösch-Zanetti, N. C.; Shih, K.-Y.; O'Donoghue, M. B.; Davis, W. M.; Reiff, W. M. *J. Am. Chem. Soc.* **1997**, *119*, 11876−11893. (e) Cooper, N. J.; Green, M. L. H. *J. Chem. Soc., Dalton Trans.* **1979**, 1121−1127.
(48) (a) Polse, J. L.; Andersen, R. A.; Bergman, R. G. *J. Am. Chem. Soc.* **1998**, *120*, 13405.
(49) Smith, M. R.; Matsunaga, P. T.; Andersen, R. A. *J. Am. Chem. Soc.* **1993**, *115*, 7049.
(50) (a) Polse, J. L.; Andersen, R. A.; Bergman, R. G. *J. Am. Chem. Soc.* **1996**, *118*, 8737−8738. (b) Kaplan, A. W.; Polse, J. L.; Ball, G. E.; Andersen, R. A.; Bergman, R. G. *J. Am. Chem. Soc.* **1998**, *120*, 11649. (c) Polse, J. L.; Kaplan, A. W.; Andersen, R. A.; Bergman, R. G. *J. Am. Chem. Soc.* **1998**, *120*, 6316.
(51) (a) Sweeney, Z. K.; Polse, J. L.; Andersen, R. A.; Bergman, R. G.; Kubinec, M. G. *J. Am. Chem. Soc.* **1997**, *119*, 4543. (b) Sweeney, Z. K.; Polse, J. L.; Andersen, R. A.; Bergman, R. G. *J. Am. Chem. Soc.* **1998**, *120*, 7825.
(52) Unit cell parameters of **9**: triclinic, *P*-1, a = 14.1509 Å, b = 20.5141 Å, c = 22.0654 Å, α = 97.156°, β = 90.062°, γ = 110.040°, Z = 4, V = 5964 Å^3. The connectivity of complex **9** is illustrated in Figure S88 in the Supporting Information.
(53) Hanna, T. E.; Keresztes, I.; Lobkovsky, E.; Bernskoetter, W. H.; Chirik, P. J. *Organometallics* **2004**, *23*, 3448−3458.
(54) Unit cell parameters of **13**: triclinic, *P*-1, a = 10.2808 Å, b = 14.8683 Å, c = 20.8162 Å, α = 97.508°, β = 103.529°, γ = 90.221°, Z = 2, V = 3065.160 Å^3. The connectivity[3] of **13** is illustrated in Figure S89 in the Supporting Information.